N71-23135

NASA TECHNICAL MEMORANDUM

NASA TM X-2162

NASA TM X-2162

CASE FILE COPY

LOW-SUBSONIC LONGITUDINAL AERODYNAMIC CHARACTERISTICS OF A TWIN-BODY SPACE-SHUTTLE BOOSTER CONFIGURATION

by Bernard Spencer, Jr., and George M. Ware

Langley Research Center
Hampton, Va. 23365

NATIONAL AERONAUTICS AND SPACE ADMINISTRATION • WASHINGTON, D. C. • APRIL 1971

1. Report No. NASA TM X-2162	2. Government Accession No.	3. Recipient's Catalog No.
4. Title and Subtitle LOW-SUBSONIC LONGITUDINAL AERODYNAMIC CHARACTERISTICS OF A TWIN-BODY SPACE-SHUTTLE BOOSTER CONFIGURATION		5. Report Date April 1971
		6. Performing Organization Code
7. Author(s) Bernard Spencer, Jr., and George M. Ware		8. Performing Organization Report No. L-7417
9. Performing Organization Name and Address NASA Langley Research Center Hampton, Va. 23365		10. Work Unit No. 124-07-24-05
		11. Contract or Grant No.
12. Sponsoring Agency Name and Address National Aeronautics and Space Administration Washington, D.C. 20546		13. Type of Report and Period Covered Technical Memorandum
		14. Sponsoring Agency Code

15. Supplementary Notes

16. Abstract

An investigation was conducted in the Langley low-turbulence pressure tunnel with a model representative of a first-stage booster space-shuttle concept proposed by industry. The configuration consisted of twin-body elements connected by fore and aft wings with each body having an outboard horizontal and a vertical stabilizer. The tests were made at angles of attack from about -4^{o} to 20^{o} at 0^{o} sideslip. Tests were made over a range of Reynolds numbers (based on body length) from 4.34×10^{6} to 26.00×10^{6} at Mach numbers below 0.35.

17. Key Words (Suggested by Author(s))		18. Distribution Statement	
Space shuttle Booster		Unclassified – Unlimited	
19. Security Classif. (of this report) Unclassified	20. Security Classif. (of this page) Unclassified	21. No. of Pages 59	22. Price* $3.00

*For sale by the National Technical Information Service, Springfield, Virginia 22151

LOW-SUBSONIC LONGITUDINAL AERODYNAMIC CHARACTERISTICS OF A TWIN-BODY SPACE-SHUTTLE BOOSTER CONFIGURATION

By Bernard Spencer, Jr., and George M. Ware
Langley Research Center

SUMMARY

An investigation has been conducted in the Langley low-turbulence pressure tunnel to determine the low-subsonic longitudinal aerodynamic characteristics of a twin-body space-shuttle booster configuration having fore and aft wings separating the bodies and outboard horizontal and vertical stabilizers. The tests were conducted at Mach numbers below 0.35 over a range of Reynolds numbers (based on body length) from 4.34×10^6 to 26.00×10^6. During the tests, the angle of attack was varied from about -4° to 20°.

Results of the investigation indicated that the model was sensitive to change in Reynolds number; for example, increasing the Reynolds number (based on body length) from 4.34×10^6 to 17.30×10^6 increased the untrimmed maximum lift-drag ratio of the minimum-span-wing model from 4.9 to 5.8. Doubling the wing span increased the maximum untrimmed lift-drag ratio from 5.8 to 8.5 but did not affect longitudinal stability or trim. The model with the fore wing in the most forward position was longitudinally unstable about the design center of gravity. Moving the fore wing rearward on the model increased longitudinal stability but did not affect lift, drag, or trim at low angles of attack. The outboard horizontal stabilizers contributed significantly to longitudinal stability and lift-drag ratio; the untrimmed lift-drag ratio of the intermediate-span-wing model was increased by an increment of about 2.0. The model had about the same longitudinal aerodynamic characteristics with the wing in either the high or low position.

INTRODUCTION

The National Aeronautics and Space Administration and industry are at present investigating, both experimentally and analytically, configurations suitable for transportation of large payloads to and from near-earth orbit. The concept as presently envisioned consists of vertically launched booster and orbiter stages which are capable of aerodynamically controlled return flight from orbit with horizontal landing capability. An investigation has been made with a preliminary conceptual booster, similar to an industry proposal, which has twin bodies and fore and aft wings separating the bodies. Outboard horizontal and vertical stabilizers were located at the base of the bodies.

The present investigation was made in the Langley low-turbulence pressure tunnel at Mach numbers below 0.35 over a range of Reynolds numbers (based on body length) from 4.34×10^6 to 26.00×10^6. The effects of both high and low wing positions were studied as well as the effects of fore wing longitudinal position, horizontal-stabilizer dihedral angle, and increasing the wing span. The investigation also included the effect of removing a portion of the trailing edge of the fore wing which simulated a closed blunt exit for cruise engines buried in the wing. The angle-of-attack range was generally from about -4° to 20° at 0° sideslip.

SYMBOLS

The longitudinal data are referred to the stability-axis system. All coefficients are normalized with respect to the actual projected planform area of a given model tested (excluding the horizontal stabilizers) and overall length of the model (constant for all configurations). Table I presents reference dimensions for the various wing-body configurations. The longitudinal location of the moment reference point was taken as 61.6 percent body length aft of the body apex, with the vertical location on the center line of the body and the lateral location at the lateral center of the configuration. (See fig. 1.) Values are given in both SI and U.S. Customary Units. The measurements and calculations were made in U.S. Customary Units.

C_D — drag coefficient, $\frac{\text{Drag}}{qS}$

C_L — lift coefficient, $\frac{\text{Lift}}{qS}$

C_m — pitching-moment coefficient, $\frac{\text{Pitching moment}}{qS l}$

L/D — lift-drag ratio

$(L/D)_{max}$ — maximum untrimmed lift-drag ratio

l — length of body, m (ft)

q — free-stream dynamic pressure, N/m^2 (lb/ft^2)

R — Reynolds number based on body length

S — projected planform area of a given configuration excluding the horizontal stabilizers, m^2 (ft^2)

α angle of attack, deg

Γ_H horizontal-stabilizer dihedral angle, positive with tip chord up, deg

Wing designations:

W_1 minimum-span wing

W_2 intermediate-span wing

W_3 maximum-span wing

APPARATUS, TESTS, AND CORRECTIONS

Tests were made in the Langley low-turbulence pressure tunnel at Reynolds numbers (based on body length) ranging from a minimum of 4.34×10^6 to a maximum of 26.00×10^6 at Mach numbers below 0.35. The angle of attack was generally varied from about -4° to 20° at 0° sideslip.

The model was supported by a single doglegged sting inserted into one of the bodies (fig. 2). The doglegged section or break point in the sting was greater than a model length behind the model base so that no forward flow or upwash interference would be expected. The balance and sting were calibrated for the effects of bending under load. The maximum deflection in roll was about 0.5° when a load of 1780 N (400 lb) was applied to the moment arm of the maximum-span wing. For all tests, total normal load was held below this value and, therefore, no corrections to model roll angle have been applied. The higher Reynolds numbers were obtained by increasing tunnel density. In all data presented, the drag represents gross drag in that base drag is included. Lift interference and tunnel blockage effects were found to be small and corrections for these have not been applied to the data.

DESCRIPTION OF MODEL

Sketches of the model are presented in figure 1 and a photograph of the high-wing model is presented as figure 2. The model consisted of twin ogive-nose cylindrical circular bodies joined by a fore wing and an aft wing. These wings were identical in planform and had symmetrical NACA 63_2A015 airfoil sections. Wings of three different spans were tested in a high and a low position; the span variations were $0.304l$, $0.456l$,

and $0.608l$ as measured between the body center lines. These wings are designated herein as W_1, W_2, and W_3, respectively. The fore wing could be moved rearward and the leading-edge longitudinal position was varied from $0.712l$ to $0.520l$ as measured from the base of the model. These fore wing positions are $0.712l$ (position 1), $0.664l$ (position 2), $0.616l$ (position 3), $0.567l$ (position 4), and $0.520l$ (position 5). In addition, a fore wing insert constituting 32.79 percent wing chord was removable from the trailing edge to simulate a closed blunt exit for cruise engines buried in the wing (fig. 1(c)). Horizontal and vertical stabilizers, identical in planform, extended outboard at the base of each body (fig. 1(a)). The stabilizers were flat plate in section with half-round leading edges and beveled trailing edges. Horizontal-stabilizer dihedral angle was 0°, 20°, or -20° (fig. 1(a)). During the investigation when the model was inverted to simulate the low wing position, the vertical tails were removed.

RESULTS AND DISCUSSION

Reynolds Number

The effects of Reynolds number on the longitudinal aerodynamic characteristics of the complete model with the minimum-span wing (W_1), the intermediate-span wing (W_2), and the maximum-span wing (W_3) are presented in figures 3, 4, and 5, respectively. In each test the Reynolds number was increased to the maximum value attainable in the wind tunnel or to a value that caused the rolling moment limit of the strain-gage balance to be reached. The lateral offset between the balance (mounted in one of the twin bodies) and the center of lift of the model resulted in much higher than usual rolling moments about the balance and, thus, became a limiting factor during the tests.

The data in figures 3 and 4 indicate that for the model with W_1 and W_2 there was no change in lift-curve slope or in stability level at low angles of attack as Reynolds number was increased. There was, however, an increase in the angle of attack for the onset of fore wing stall, which resulted in improved drag due to lift, and an increase in maximum untrimmed lift-drag ratio. Above a Reynolds number of 17.30×10^6 for the W_1 configuration (fig. 3) and 13.90×10^6 for the W_2 configuration (fig. 4), there was essentially no change in aerodynamic characteristics. The untrimmed maximum lift-drag ratio was increased from 4.9 to 5.8 for the W_1 configuration and from 6.3 to 7.3 for the W_2 configuration by increasing the Reynolds number from 4.34×10^6 to 17.30×10^6. The highest Reynolds number possible for the maximum-span wing (W_3) was 13.00×10^6 because of the rolling moment limitation. The data for this configuration (fig. 5) show that, although the most significant changes due to Reynolds number had occurred by $R = 13.00 \times 10^6$, the maximum lift-drag ratio was still increasing and the break in the lift-coefficient, drag-coefficient, and pitching-moment-coefficient curves was occurring at increasingly higher angles of attack which indicated that full leading-edge suction had not been reached.

In addition, the maximum angle of attack for the onset of wing stall had not been attained. Therefore, the data presented for the W_3 configuration are believed to be conservative at the higher angles of attack. The value of $(L/D)_{max}$ for this configuration was increased over the Reynolds number range of the tests from 7.6 to 8.5 (fig. 5).

Wing Span

The effects of wing span on the longitudinal aerodynamic characteristics of the model are shown in figure 6. The data are plotted for the nearest test Reynolds number below that value at which no change in aerodynamic characteristics occurred in an attempt to present data for each wing configuration at approximately the same effective Reynolds number.

The data show the expected effects of an increase in aspect ratio, namely, an increase in lift-curve slope, an increase in untrimmed lift-drag ratio due to the improved drag due to lift, and a small change in low-lift longitudinal stability.

Wing Position

The effects of low and of high wing position on the model with W_1, W_2, and W_3 are presented in figure 7. The low wing position was simulated by inverting the basic (high wing) model and testing it through the same angle-of-attack range as that used in the investigation of the high wing position. Also, since the basic model had provision for only upper surface vertical stabilizers, the comparison of the data for the high and low wing position was made with the vertical stabilizers off. The data for the high and low wing positions were obtained at different Reynolds numbers and are therefore comparable only at the lower angles of attack. As may be determined from figure 7, the longitudinal aerodynamic characteristics of the two configurations were quite similar. The lift-curve slopes for the high-wing model as wing span is increased were, however, slightly higher than those for the low-wing model but there was essentially no difference in the level of longitudinal stability. The lift-drag ratios for the two configurations, although not directly comparable, were not significantly different.

Longitudinal Position of Fore Wing

The effects of moving the fore wing from wing leading-edge position 1 to position 5 on the three wing-span configurations (W_1, W_2, W_3) with and without fore wing insert are presented in figures 8 to 10. The data indicate that for the wing insert in, longitudinal position of the fore wing had no appreciable effect on the lift and drag characteristics of the model. The longitudinal stability was increased as the wing was moved rearward. The model with the fore wing in the most forward position was unstable (static margin of -5 to -6 percent body length) about the design center of gravity at 61.6 percent body length

and became stable (static margin of about +2 percent body length) only at the most rearward position tested. (See figs. 8(a), 9(a), and 10(a).)

Fore Wing Insert Out

Reducing the wing area ahead of the center of gravity by removing the trailing edge of the fore wing increased the longitudinal stability for all fore wing longitudinal positions tested. (See figs. 8 to 10.) The model, however, was still unstable with the fore wing in the most forward position. Removing the fore wing insert also resulted in a loss in untrimmed $(L/D)_{max}$ for all configurations.

Horizontal Stabilizers and Stabilizer Dihedral Angle

The effects of horizontal stabilizers and stabilizer dihedral angle on the longitudinal aerodynamic characteristics of the model with W_2 in high position and fore wing in longitudinal position 3 are presented in figure 11. Comparison of the data for model with and without horizontal stabilizers indicates that the stabilizers were very effective in increasing longitudinal stability and contributed significantly to increasing the lift-curve slope and untrimmed lift-drag ratio (an increase in untrimmed $(L/D)_{max}$ of about 2). Changing the horizontal-stabilizer dihedral angle from the initial 0° to 20° or -20° resulted in only minor differences in the basic longitudinal aerodynamic characteristics of the model.

SUMMARY OF RESULTS

Wind-tunnel tests have been made to determine the low-subsonic longitudinal aerodynamic characteristics of a twin-body booster configuration having fore and aft wings separating the bodies. The configuration also had outboard vertical and horizontal stabilizers at the base of each body. The results of the investigation may be summarized as follows:

1. The model was sensitive to change in Reynolds number; for example, increasing the Reynolds number (based on body length) from 4.34×10^6 to 17.30×10^6 increased the untrimmed maximum lift-drag ratio of the minimum-span-wing model from 4.9 to 5.8.

2. Doubling the wing span of the model increased the maximum untrimmed lift-drag ratio from 5.8 to 8.5 but did not affect longitudinal stability or trim.

3. Longitudinal instability about the design center of gravity was noted for the model with the fore wing in the most forward position. Moving the fore wing rearward stabilized the model without affecting lift, drag, or trim at low angles of attack.

4. The horizontal stabilizers were very effective in increasing longitudinal stability and contributed significantly to increasing the lift-curve slope and untrimmed lift-drag ratio (an increase of about 2).

5. The model had about the same longitudinal aerodynamic characteristics with the wing in either the high or low position.

Langley Research Center,
National Aeronautics and Space Administration,
Hampton, Va., February 25, 1971.

TABLE I.- REFERENCE DIMENSIONS FOR WING-BODY CONFIGURATIONS

Wing	Area, S		Body length, l	
	m^2	ft^2	m	ft
Minimum-span wing (W_1):				
Insert in	0.09308	1.00191	0.52831	1.73333
Insert out	0.08630	0.92900	0.52831	1.73333
Intermediate-span wing (W_2):				
Insert in	0.10862	1.16920	0.52831	1.73333
Insert out	0.09526	1.02540	0.52831	1.73333
Maximum-span wing (W_3):				
Insert in	0.12417	1.33660	0.52831	1.73333
Insert out	0.10408	1.12028	0.52831	1.73333

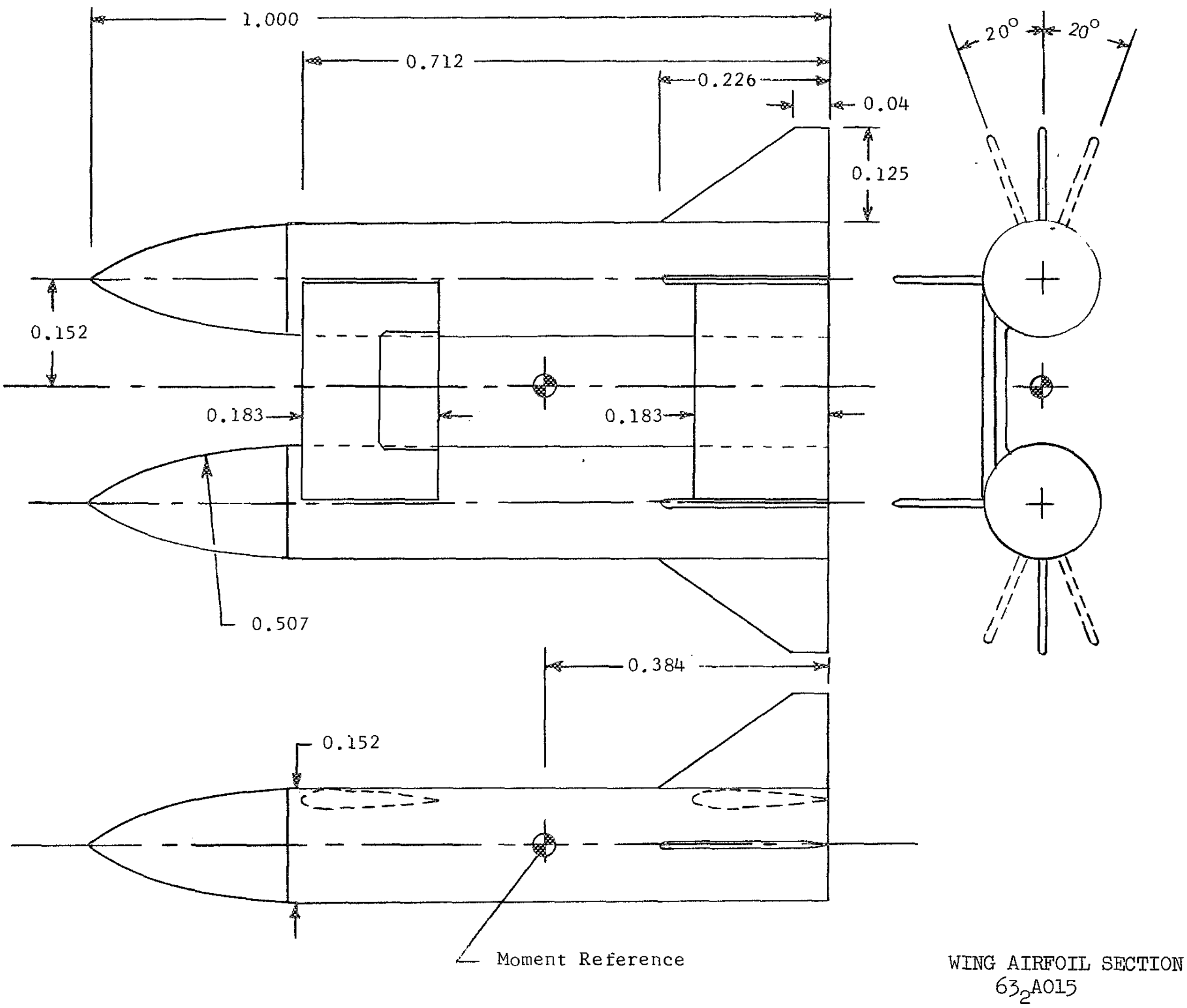

(a) Model with wing 1.

Figure 1.- Sketches of model used in investigation. All dimensions are normalized with respect to a body length of 52.8 centimeters (20.8 inches).

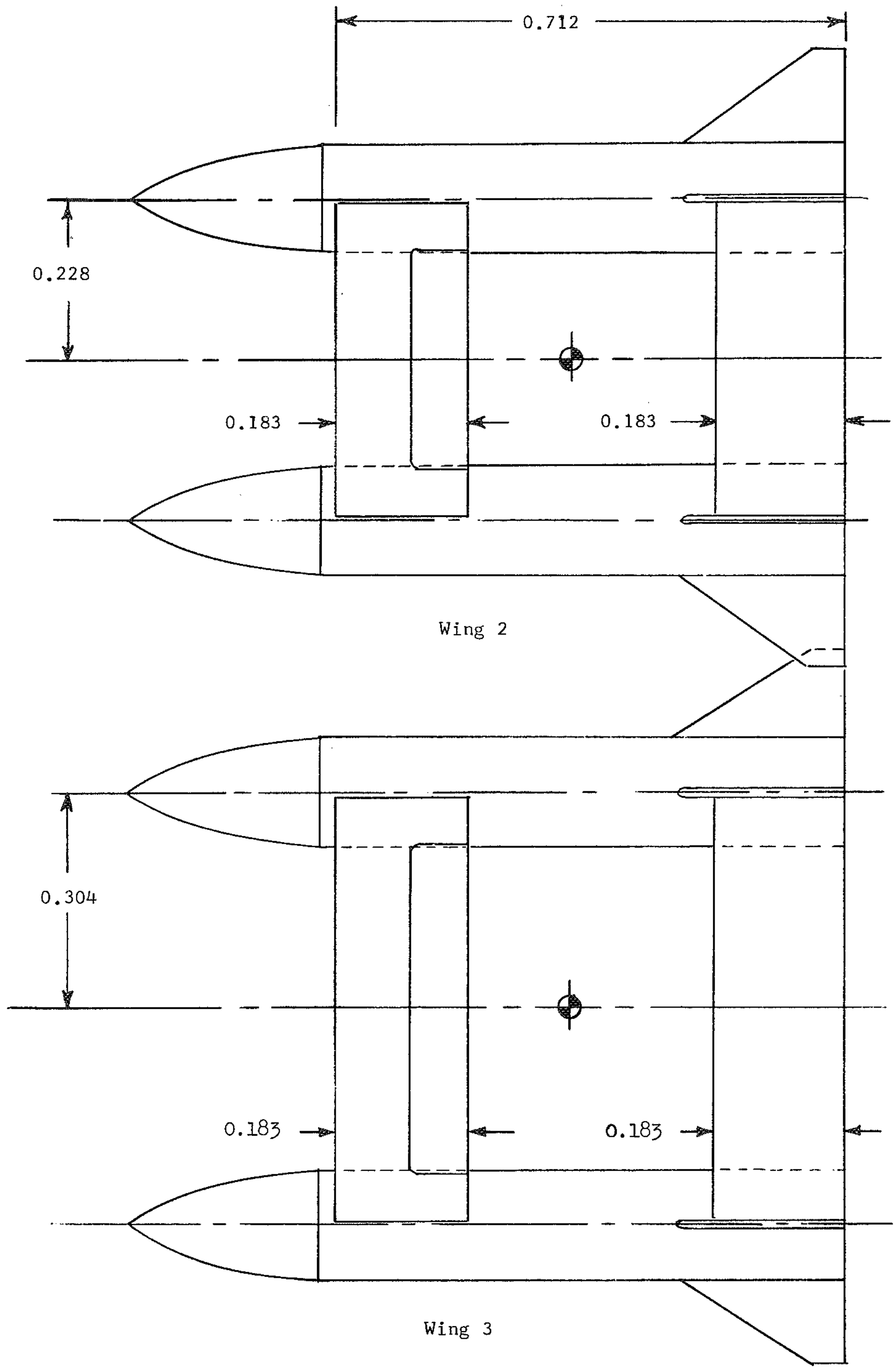

(b) Model with wings 2 and 3.

Figure 1.- Continued.

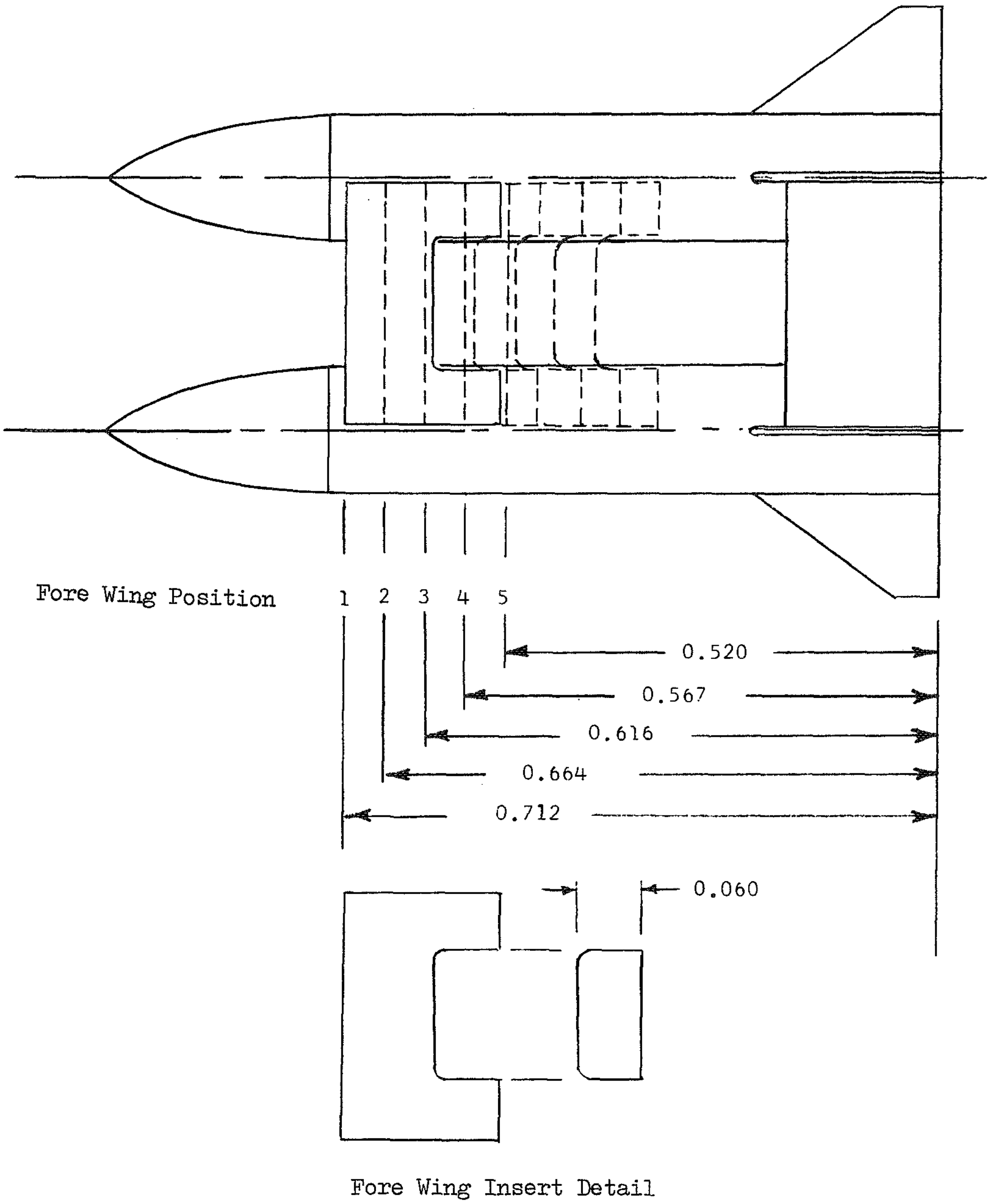

(c) Fore wing positions.

Figure 1.- Concluded.

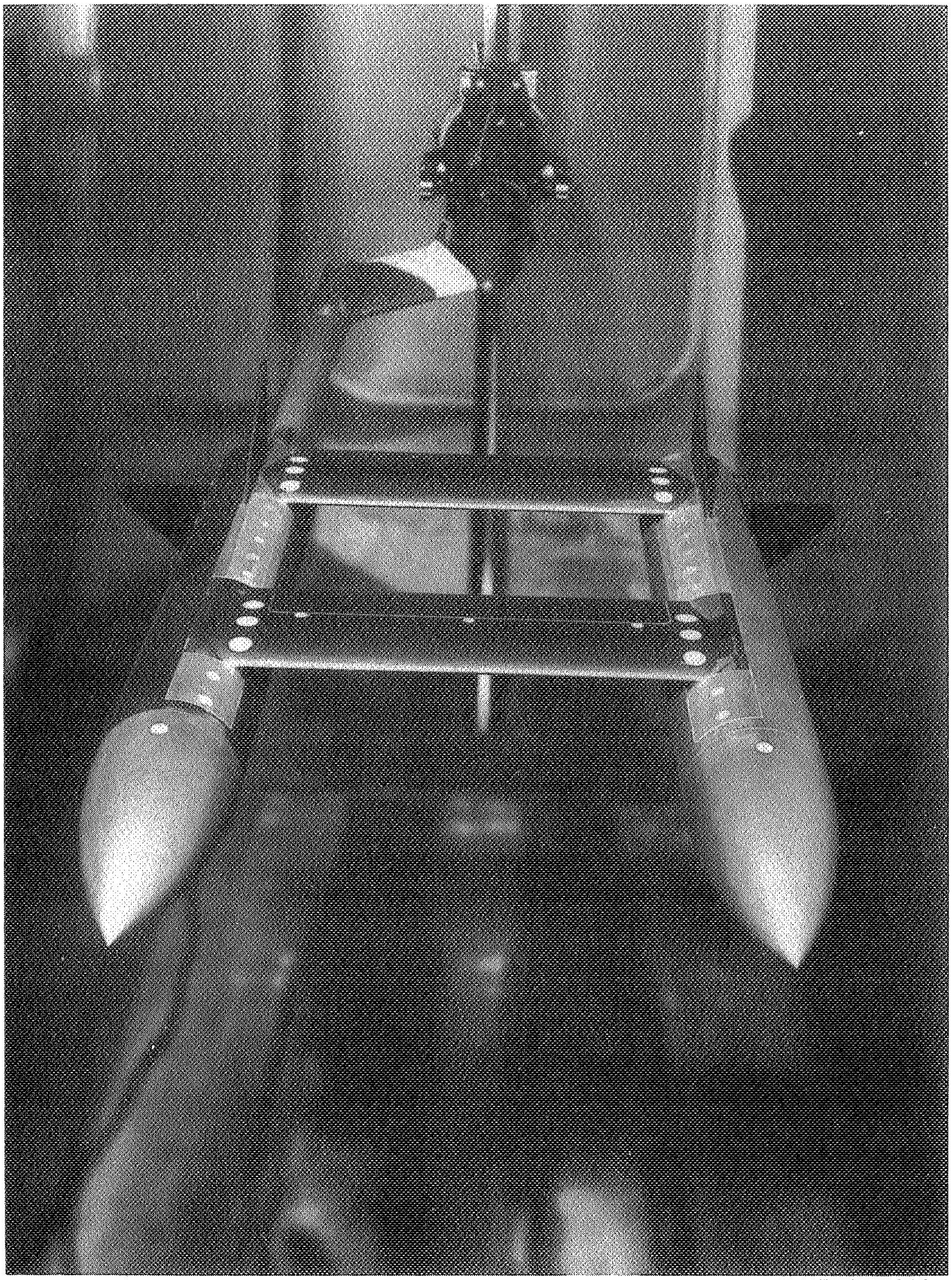

L-70-2692

Figure 2.- High-wing model mounted in Langley low-turbulence pressure tunnel.

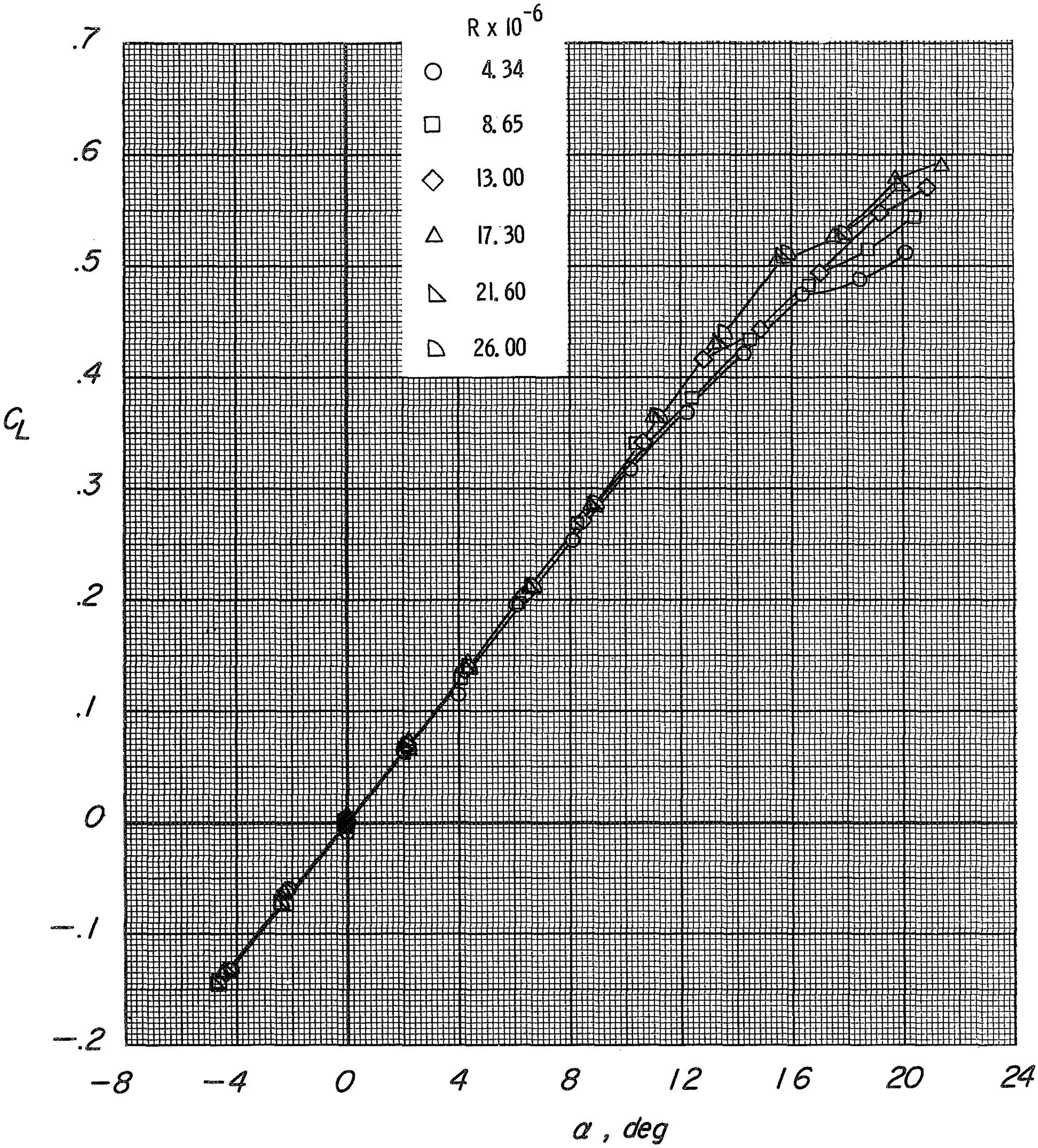

Figure 3.- Effects of Reynolds number on longitudinal aerodynamic characteristics of model with minimum-span wings (W_1) in high position. Fore wing in longitudinal position 1; vertical tails on; $\Gamma_H = 0^{\circ}$.

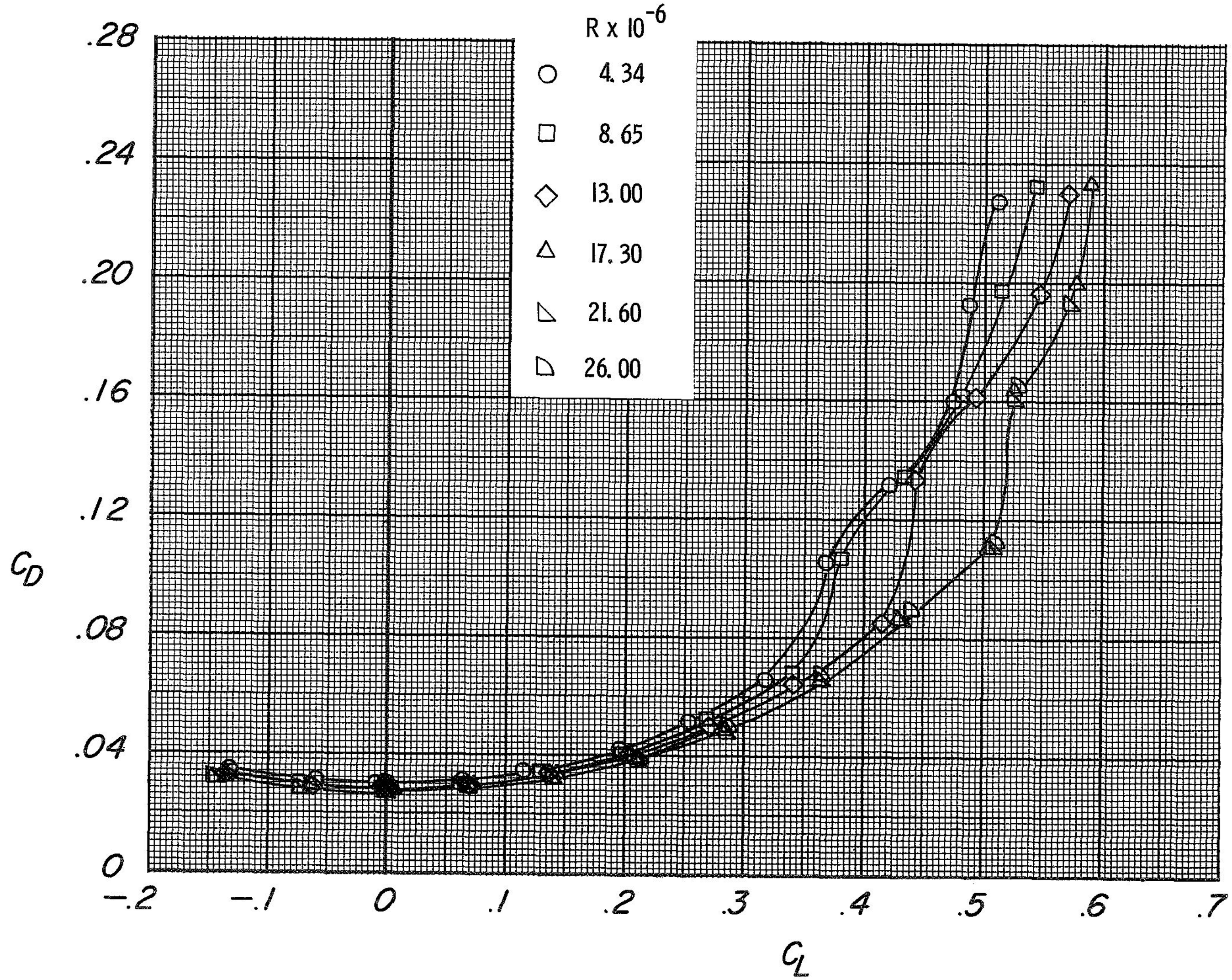

Figure 3.- Continued.

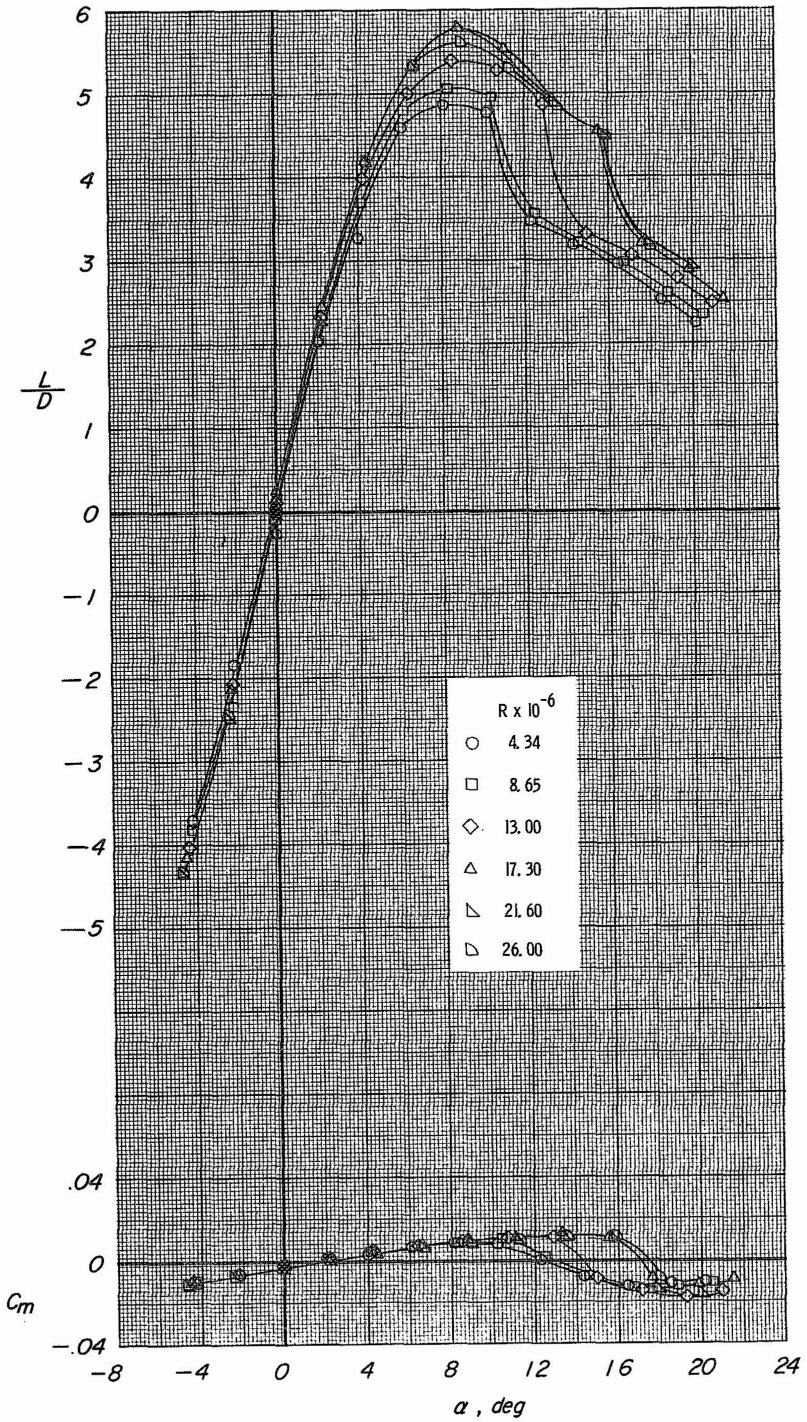

Figure 3.- Continued.

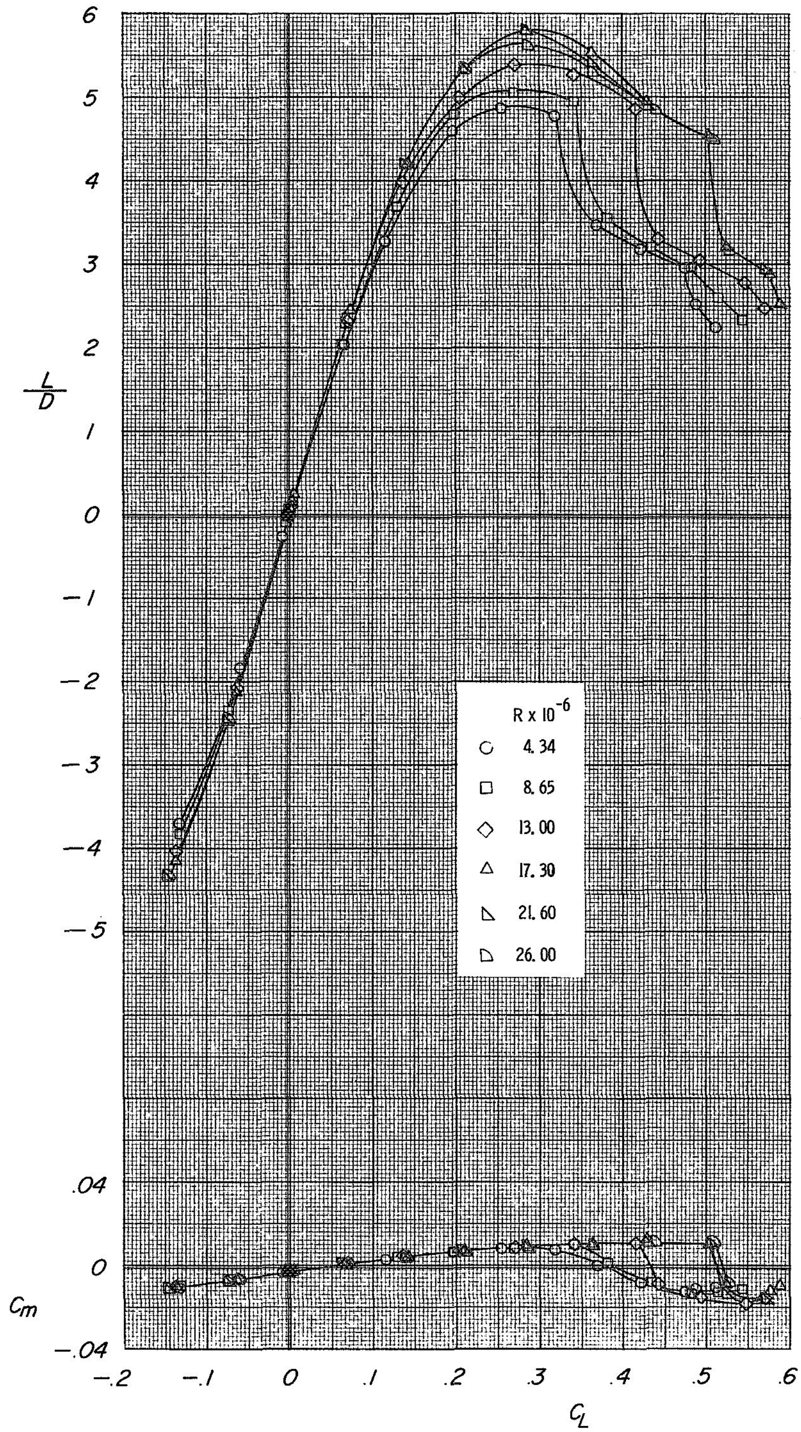

Figure 3.- Concluded.

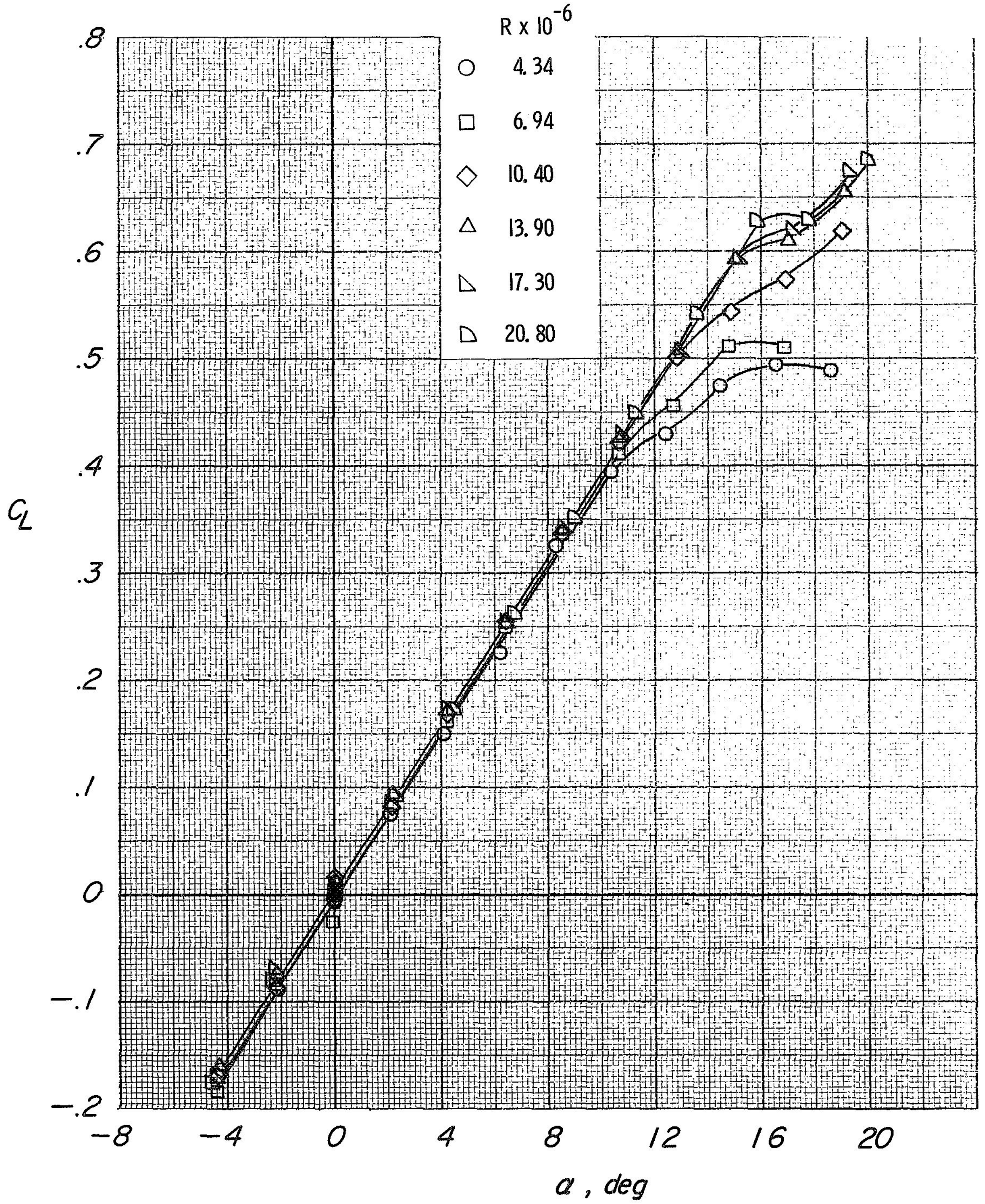

Figure 4.- Effects of Reynolds number on longitudinal aerodynamic characteristics of model with intermediate-span wings (W_2) in high position. Fore wing in longitudinal position 1; vertical tails on; $\Gamma_H = 0^o$.

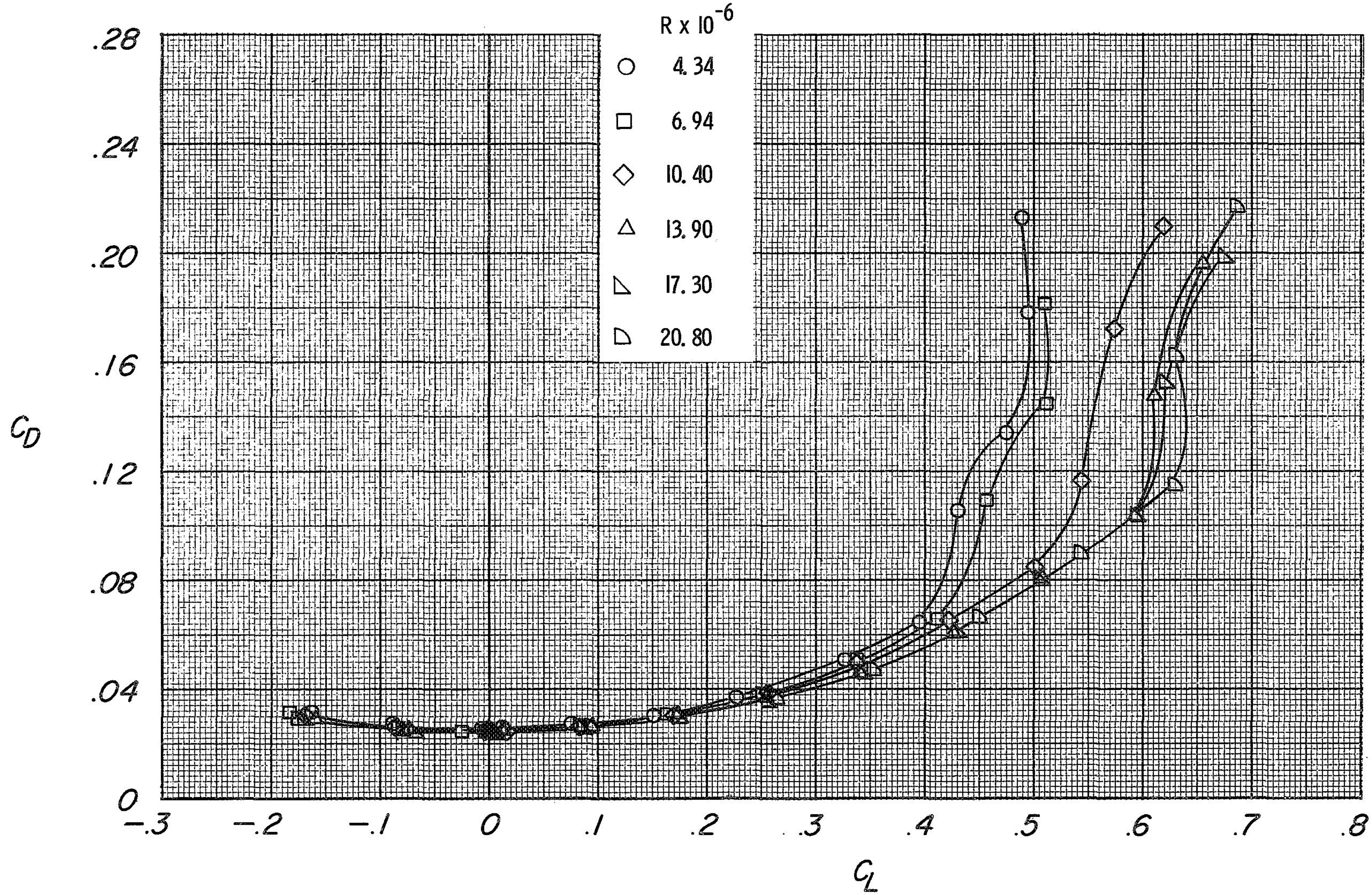

Figure 4.- Continued.

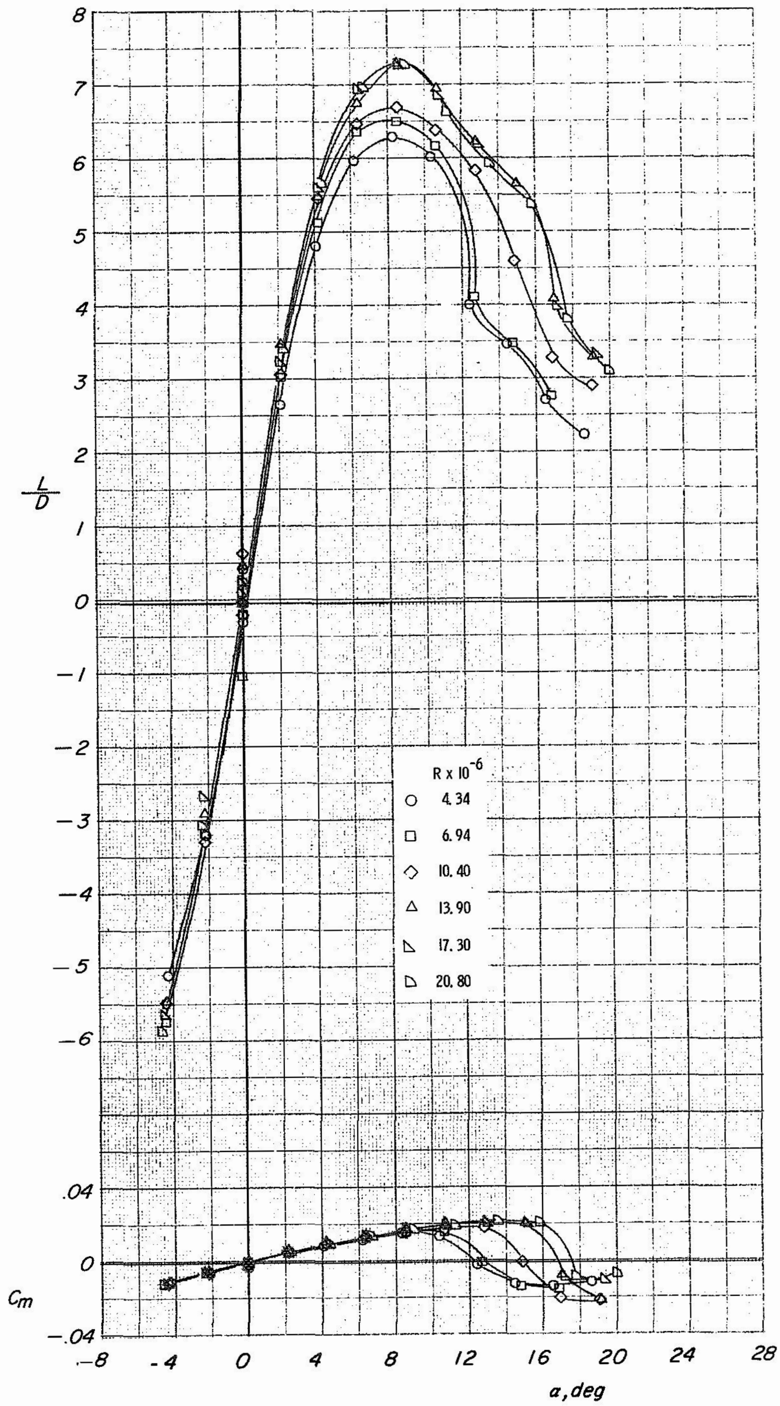

Figure 4.- Continued.

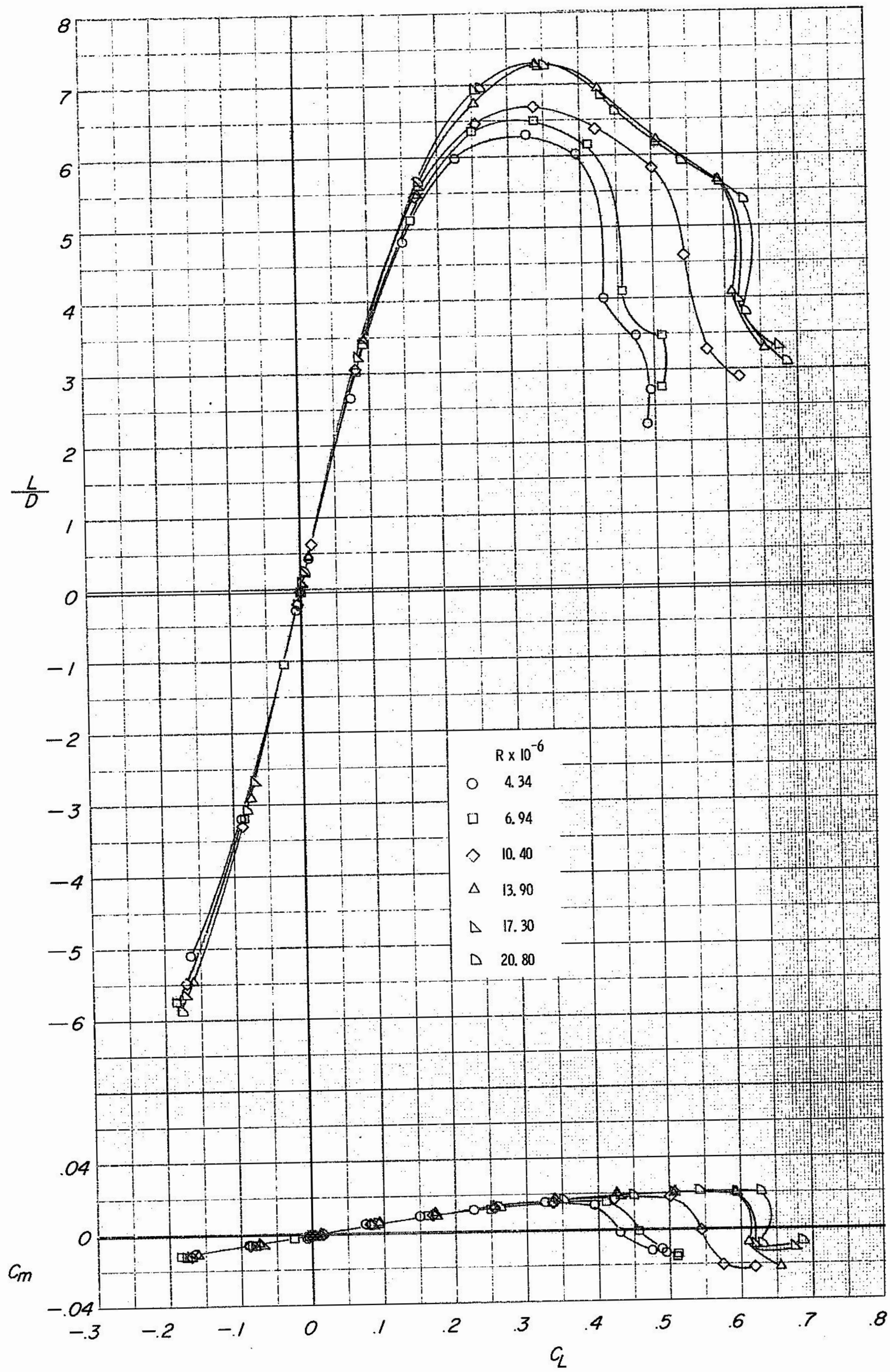

Figure 4.- Concluded.

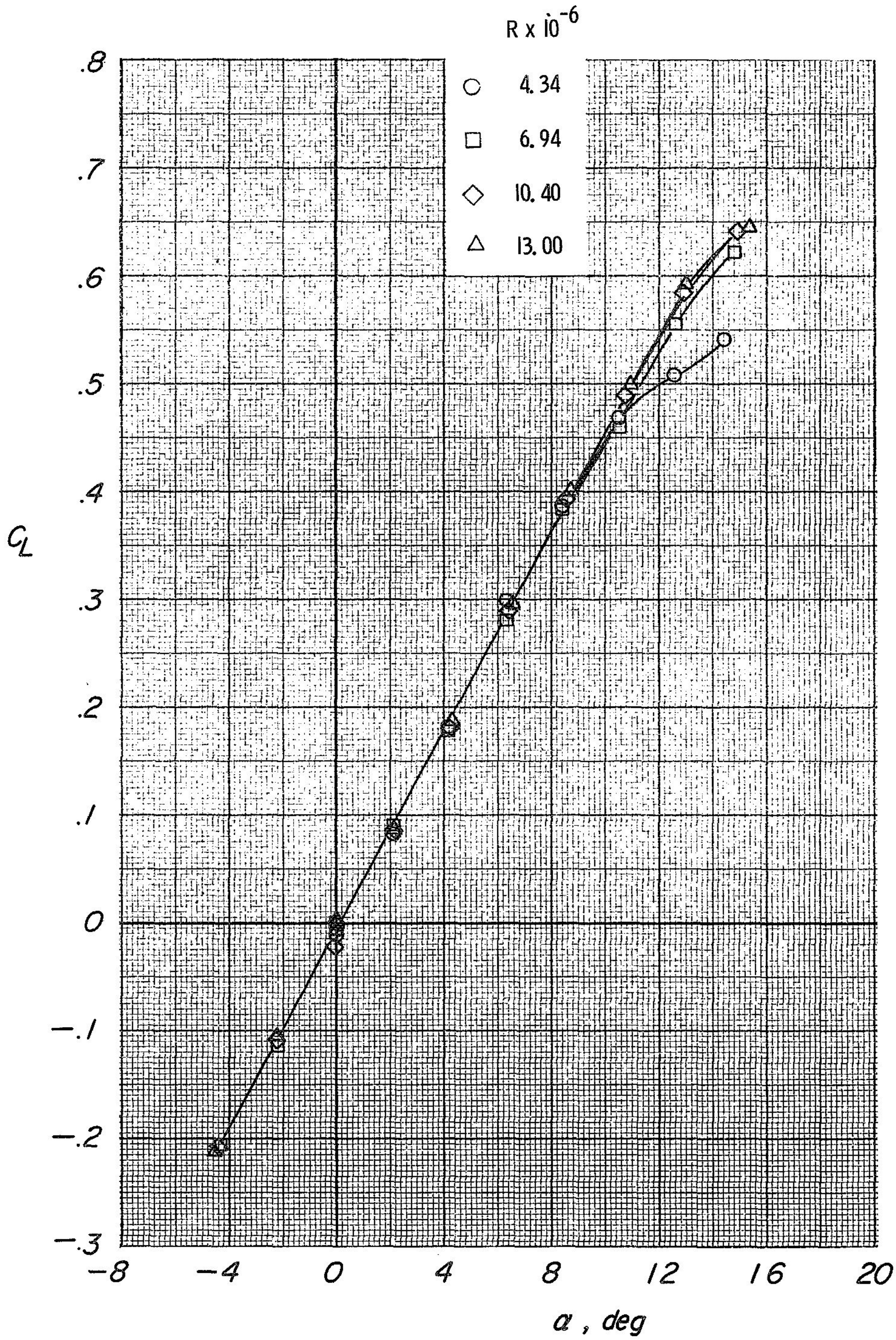

Figure 5.- Effects of Reynolds number on longitudinal aerodynamic characteristics of model with maximum-span wings (W_3) in high position. Fore wing in longitudinal position 1; vertical tails on; $\Gamma_H = 0^{\circ}$.

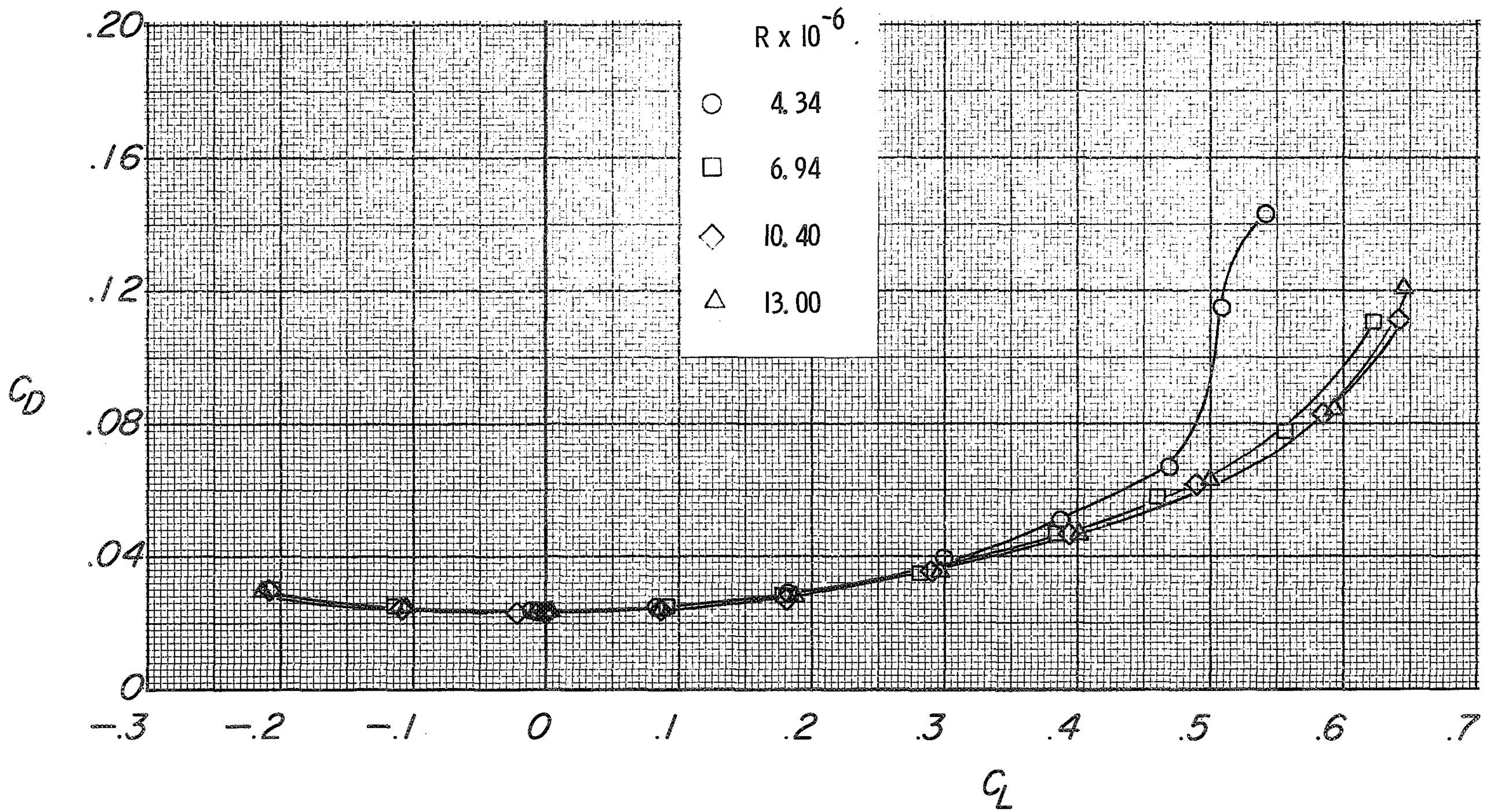

Figure 5.- Continued.

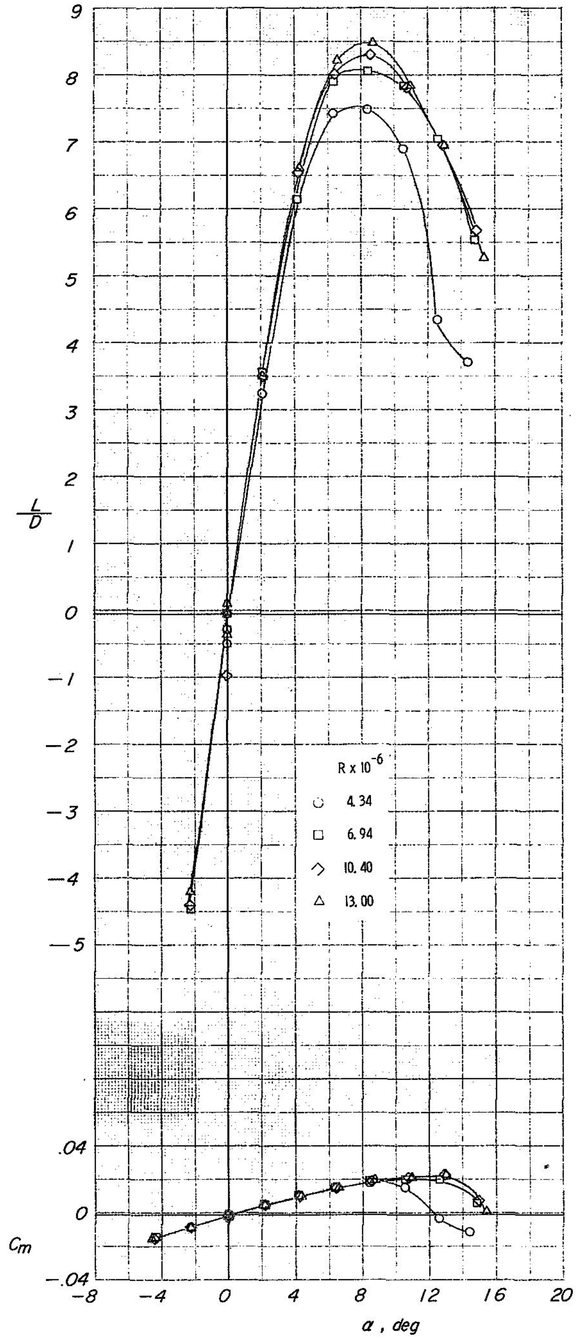

Figure 5.- Continued.

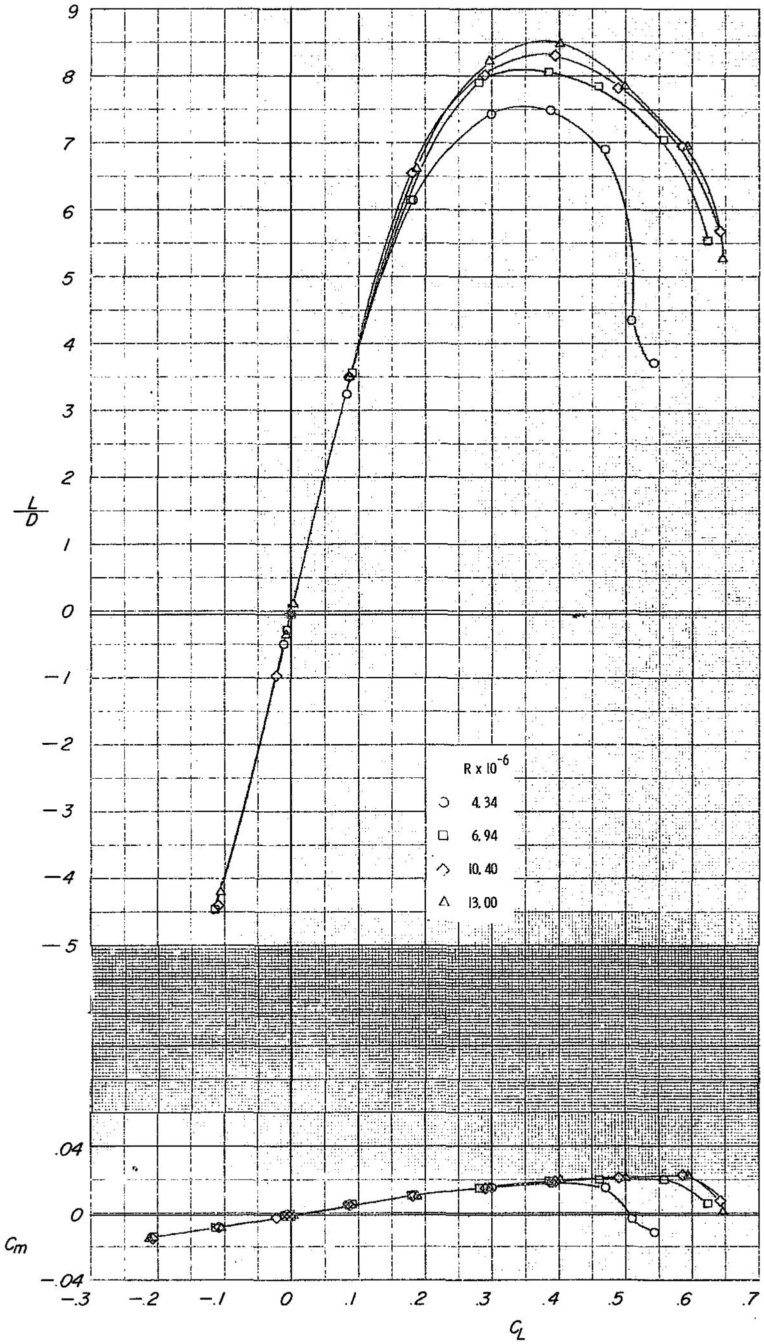

Figure 5.- Concluded.

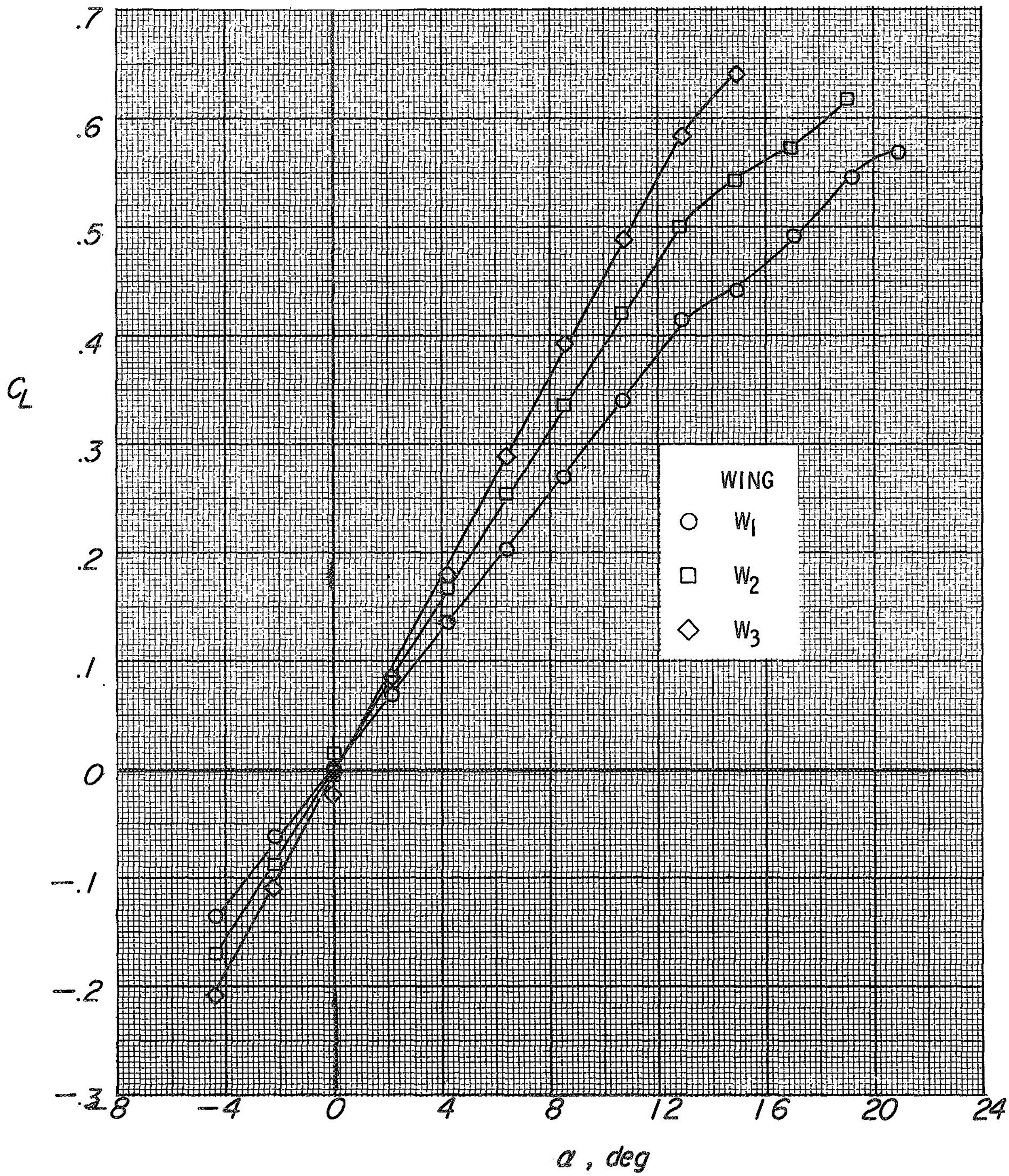

Figure 6. - Effects of wing span on longitudinal aerodynamic characteristics of model with wings in high position. Fore wing in longitudinal position 1; vertical tails on; $\Gamma_H = 0^{\circ}$.

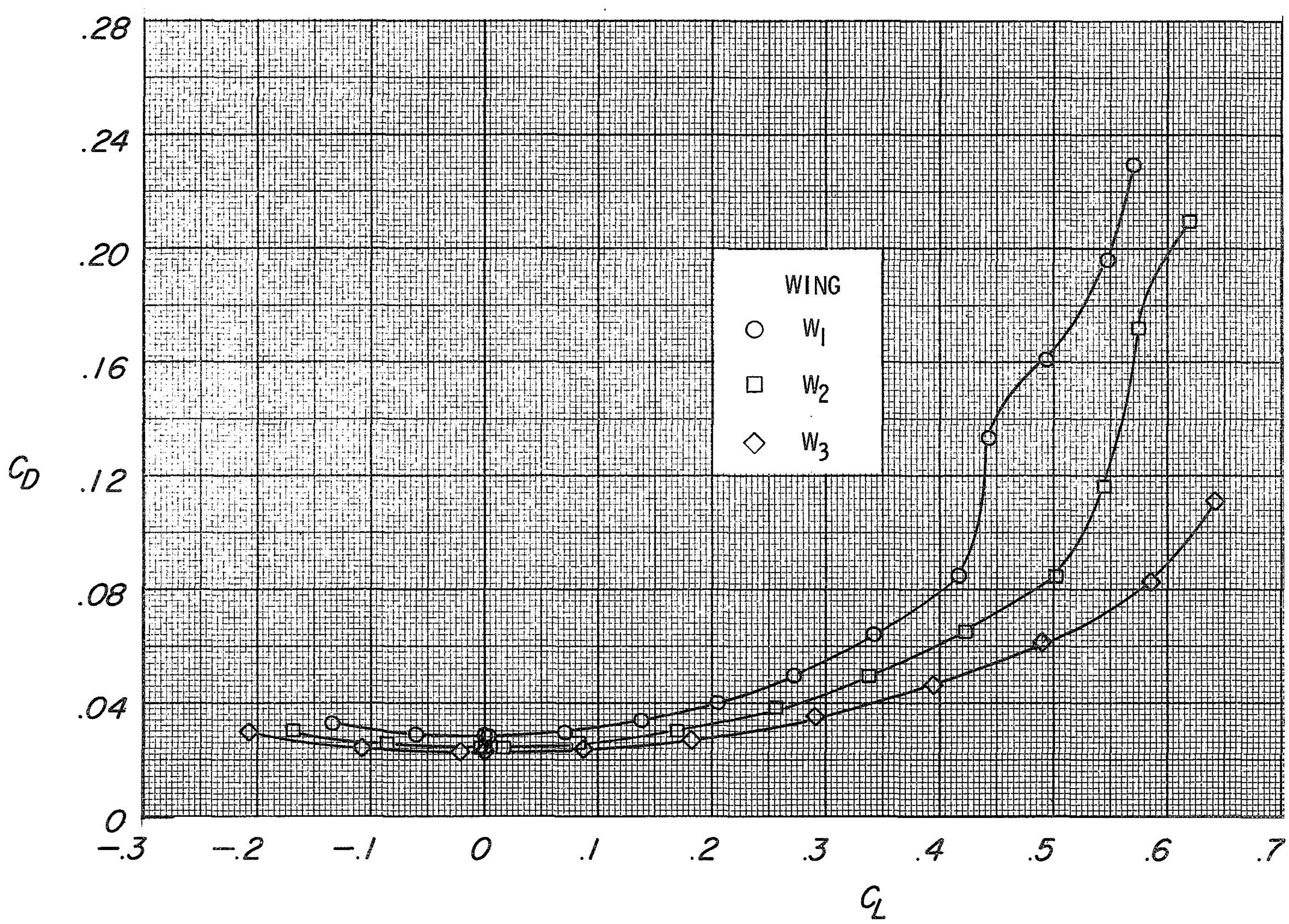

Figure 6.- Continued.

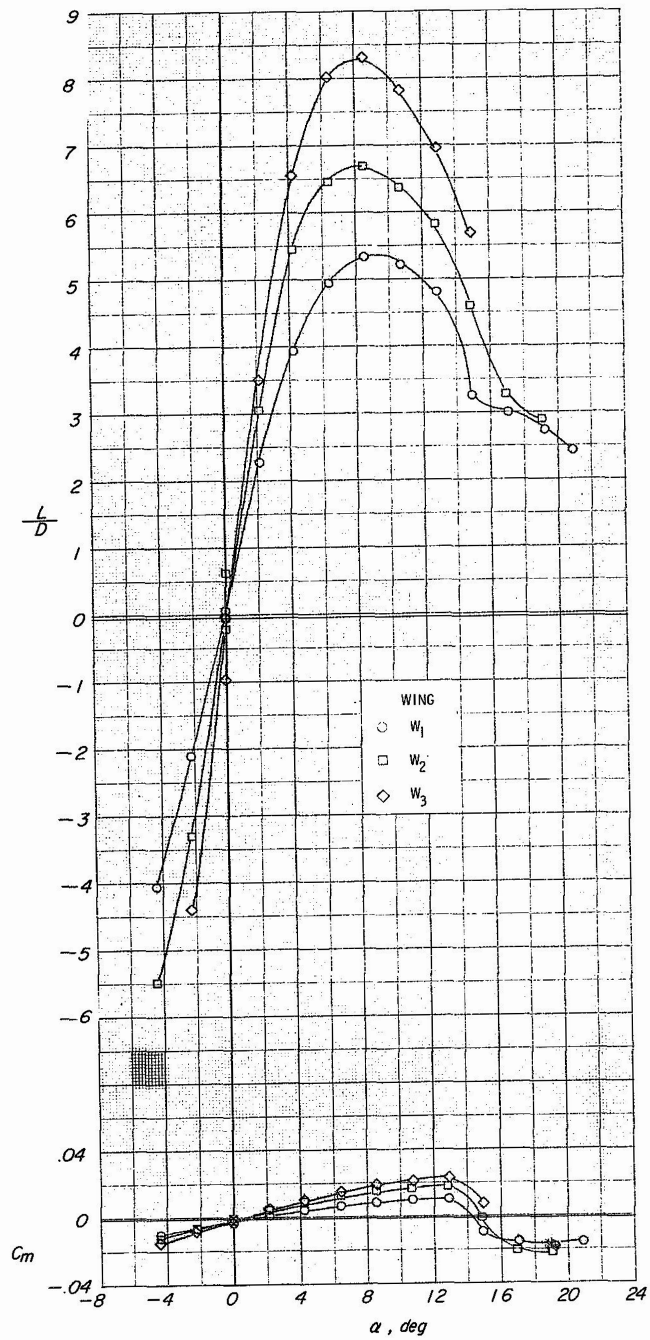

Figure 6.- Continued.

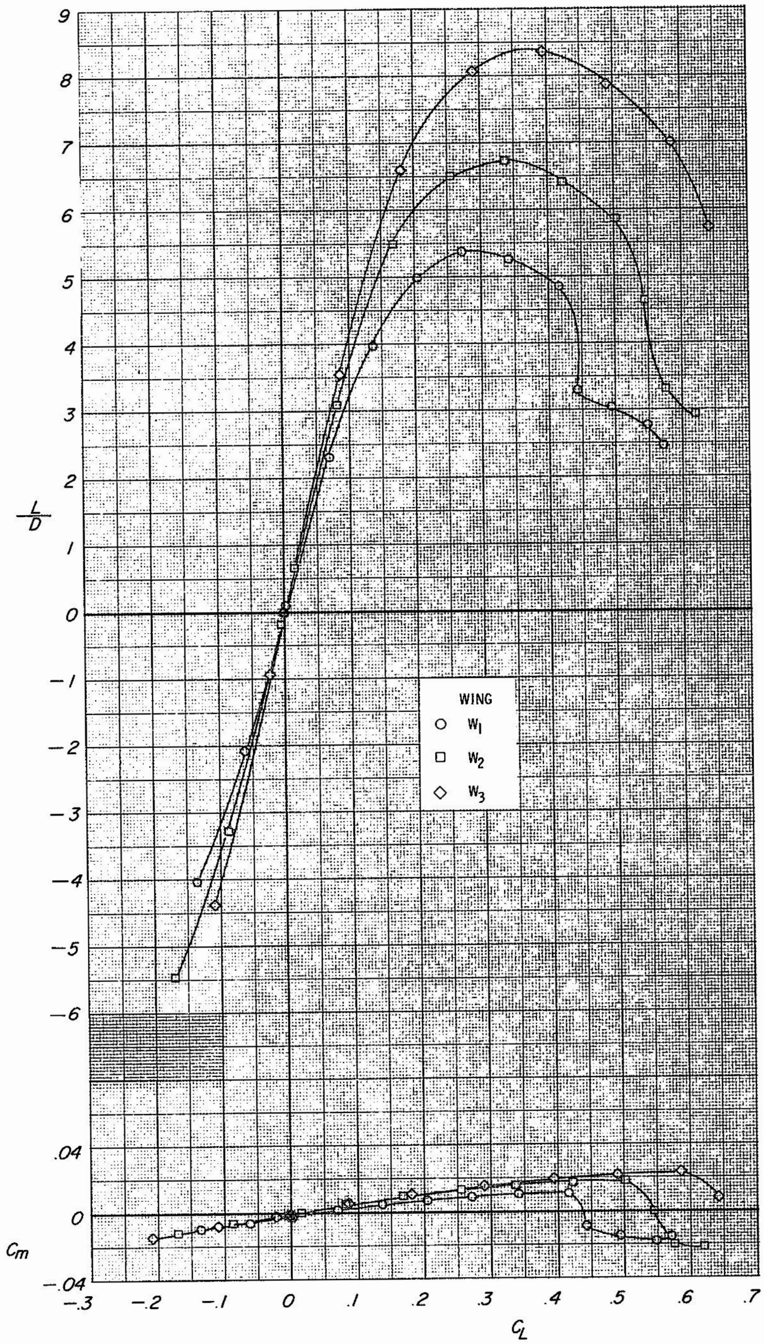

Figure 6.- Concluded.

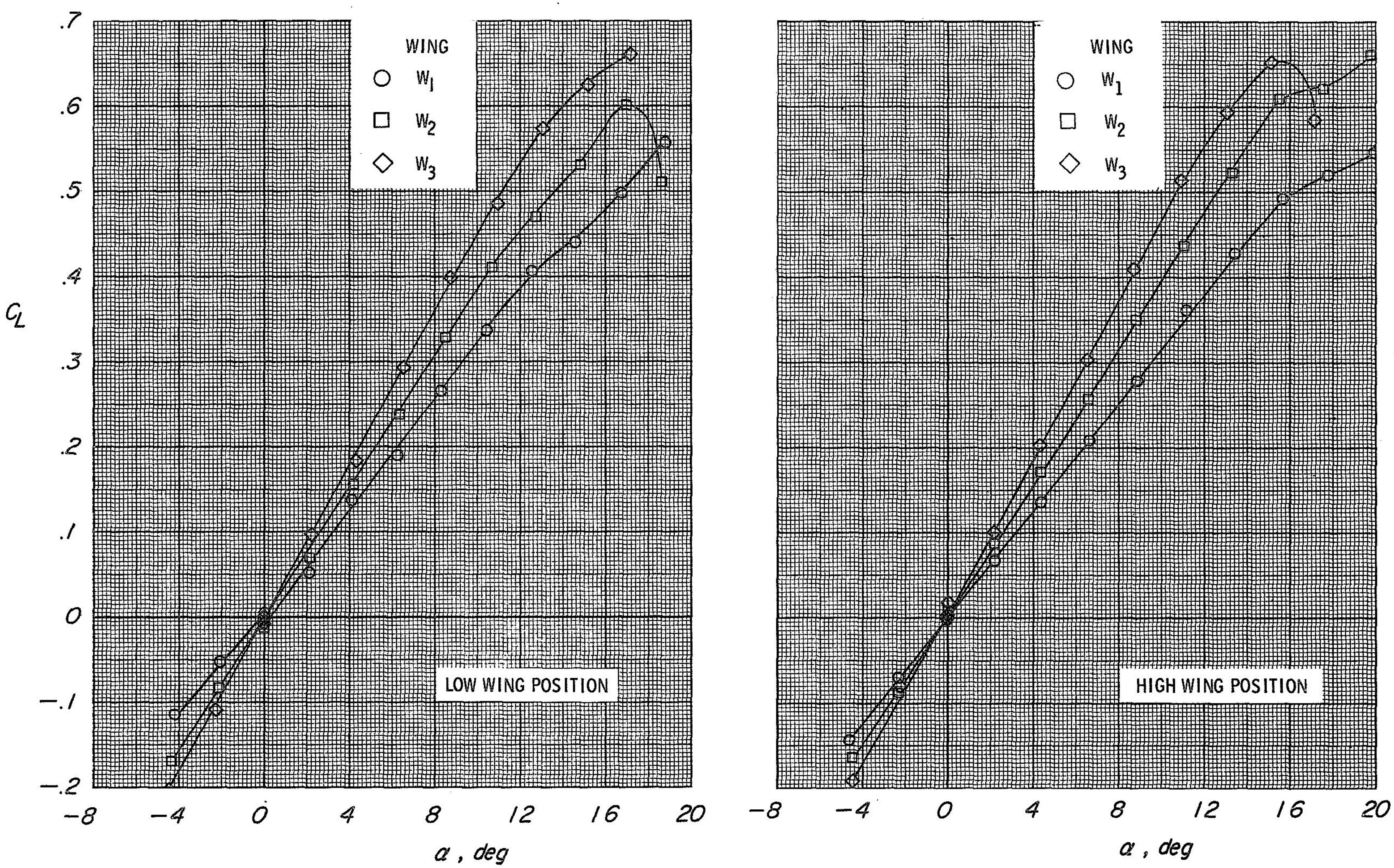

Figure 7.- Effects of wing span and wing position on the longitudinal aerodynamic characteristics of model. R = 10.4×10^6; fore wing in longitudinal position 3; vertical tails off; $\Gamma_H = 0^o$.

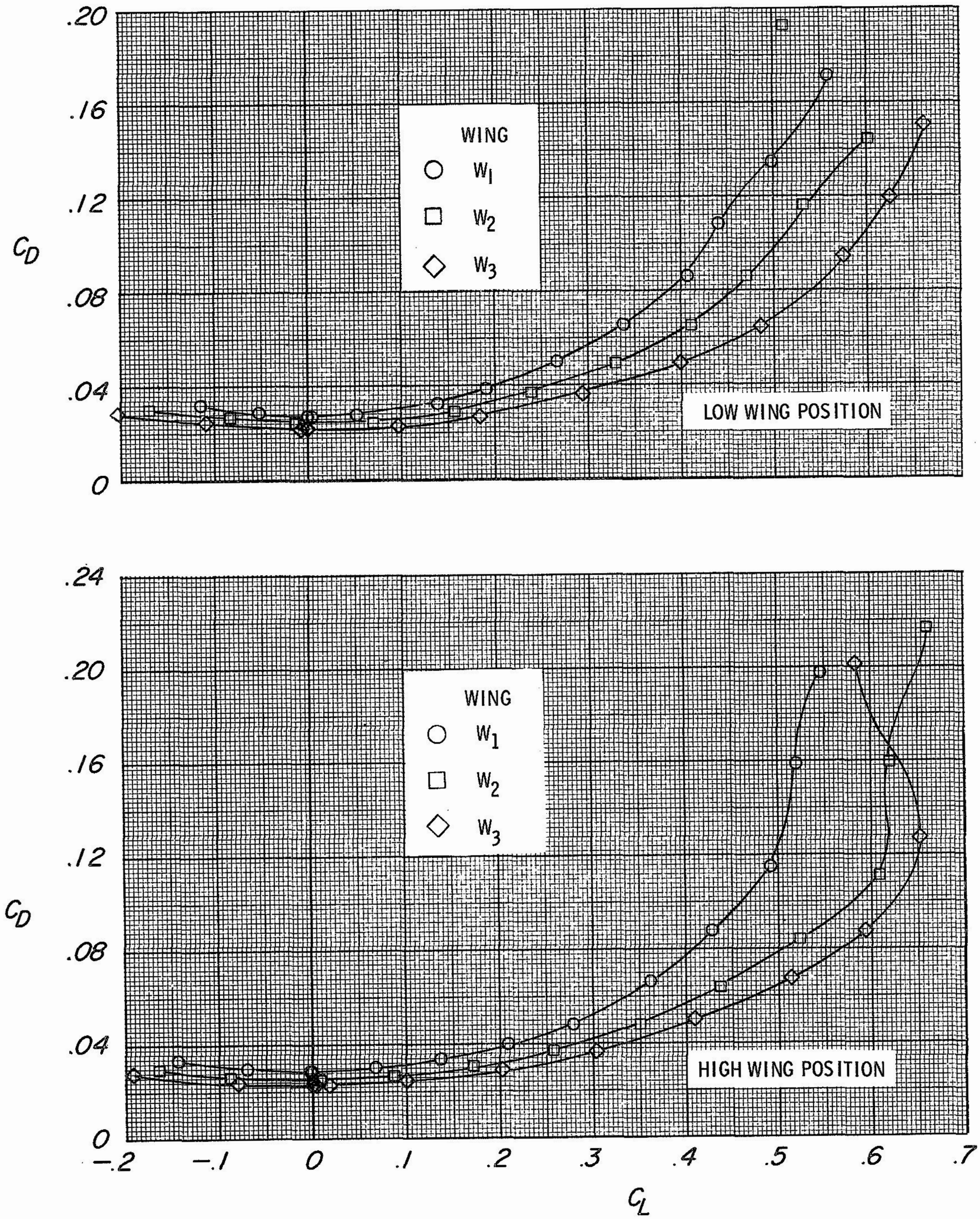

Figure 7.- Continued.

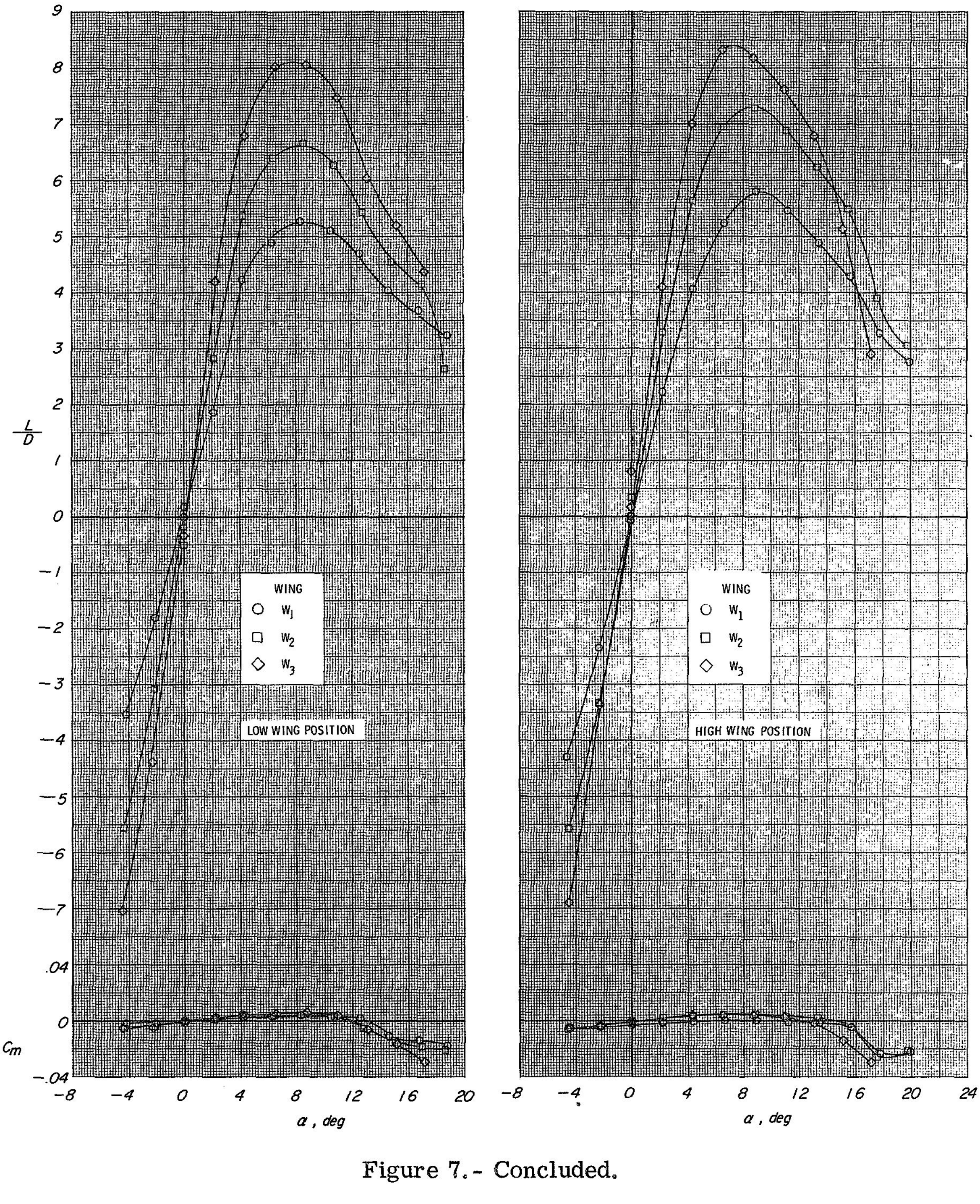

Figure 7.- Concluded.

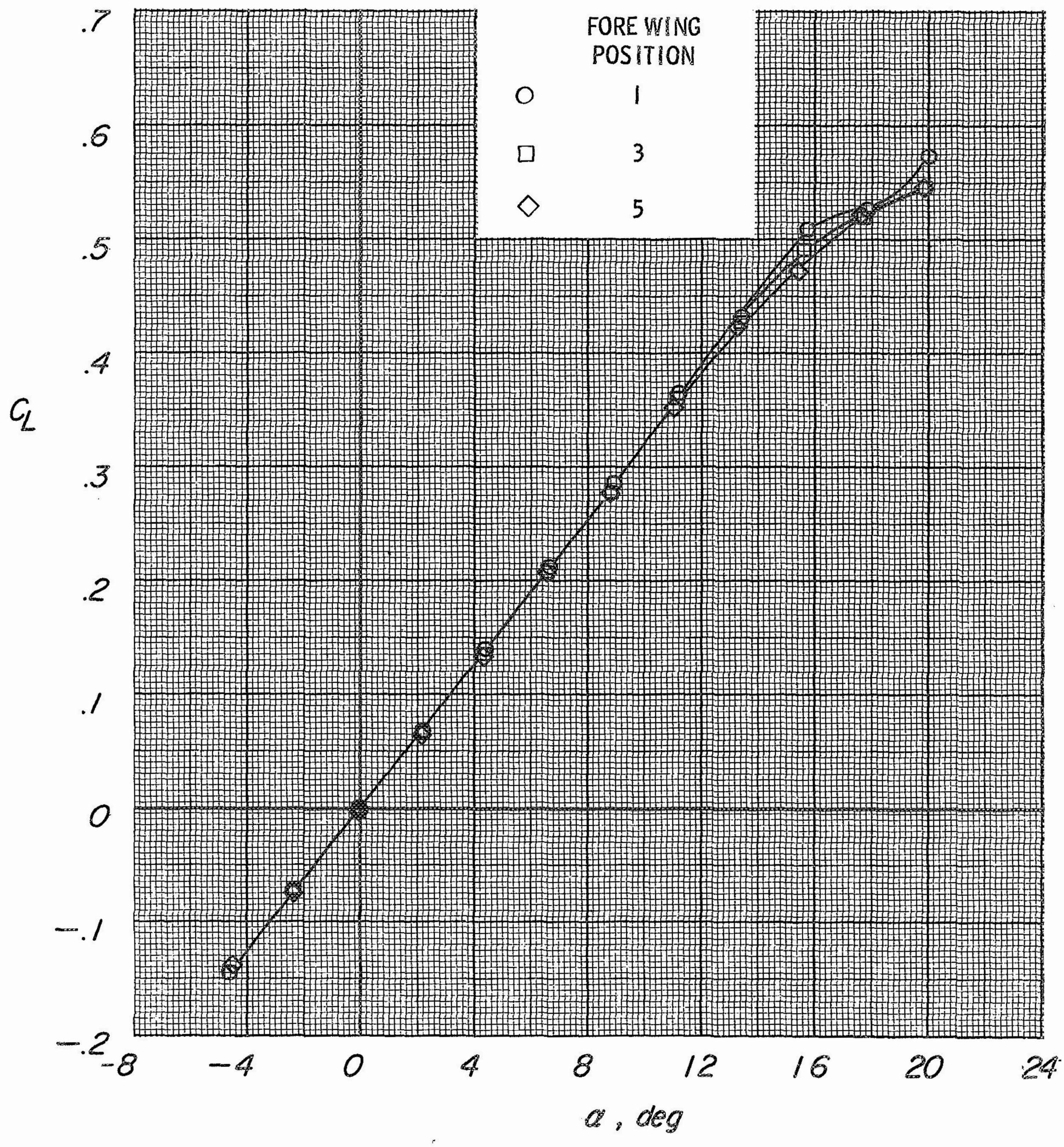

(a) Fore wing insert in.

Figure 8.- Effects of fore wing longitudinal position on longitudinal aerodynamic characteristics of model with minimum-span wings (W_1) in high position. $R = 21.6 \times 10^6$; vertical tails on; $\Gamma_H = 0^\circ$.

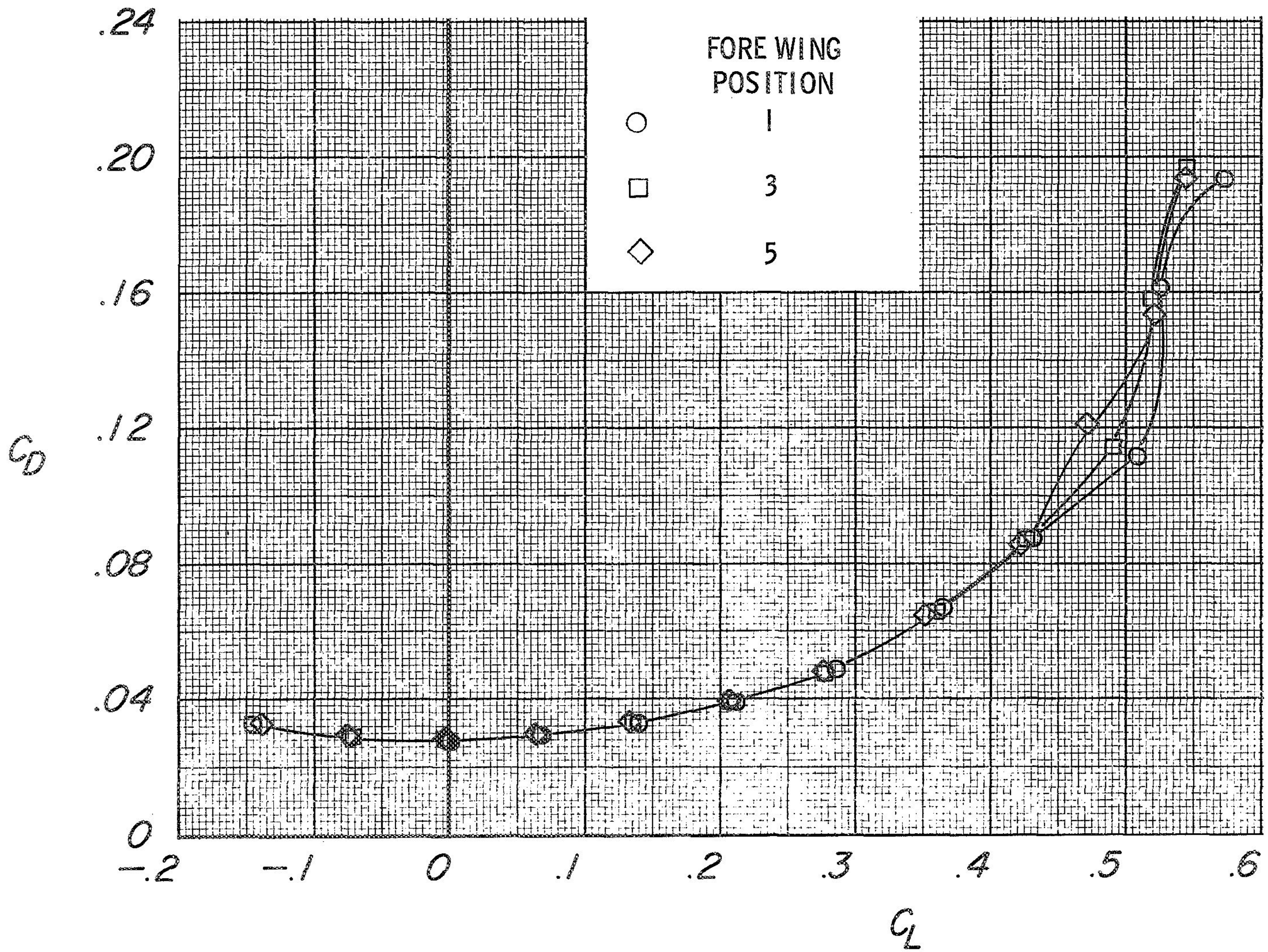

(a) Continued.

Figure 8.- Continued.

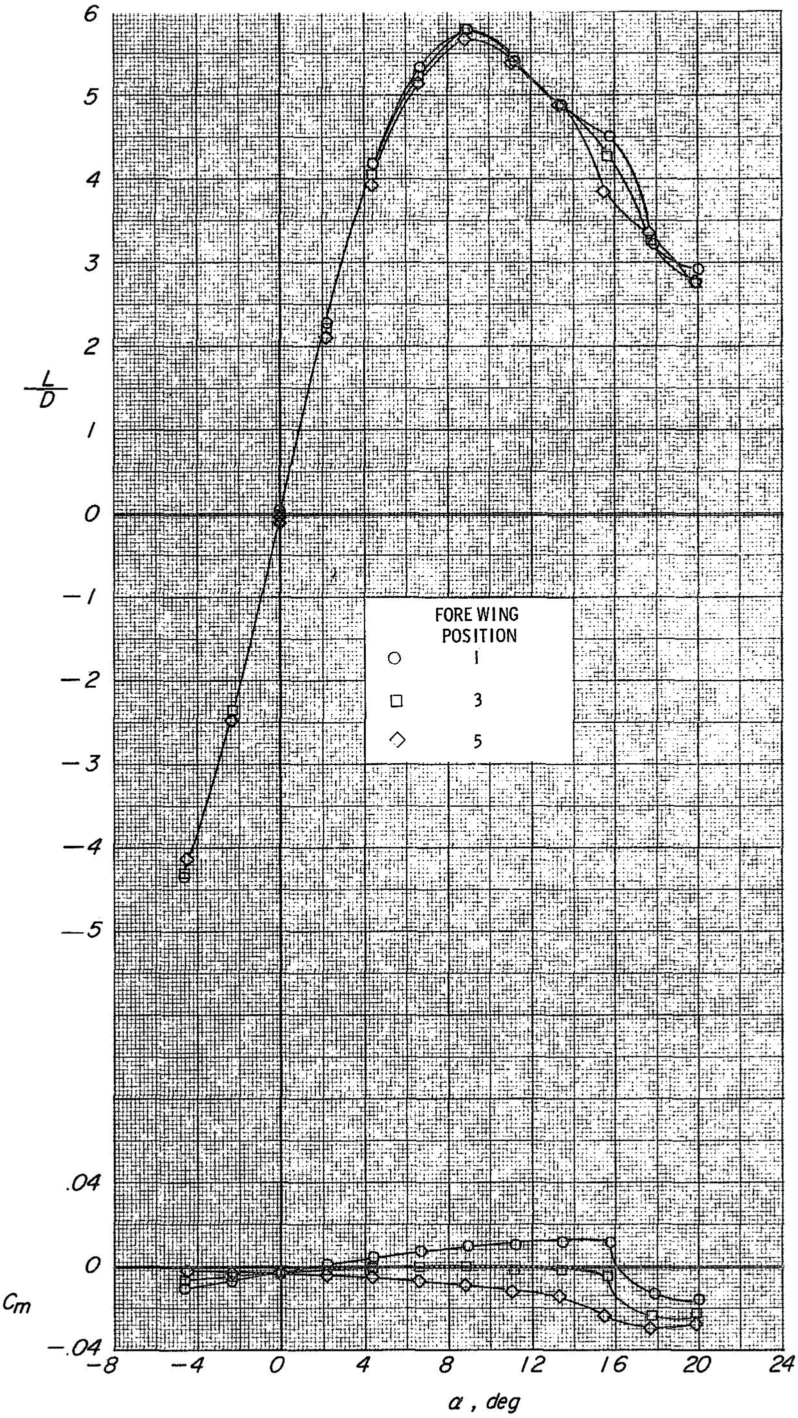

(a) Continued.

Figure 8.- Continued.

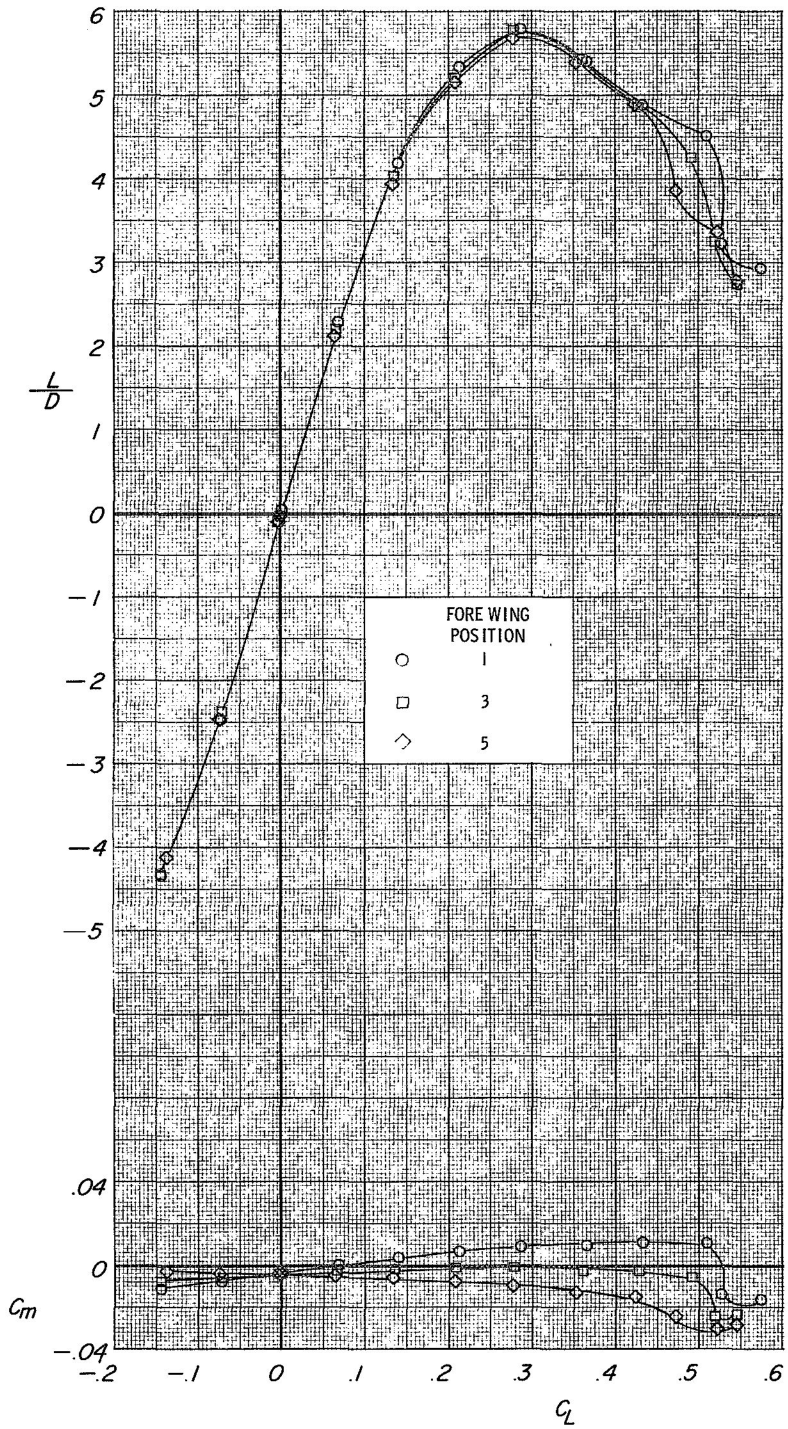

(a) Concluded.

Figure 8.- Continued.

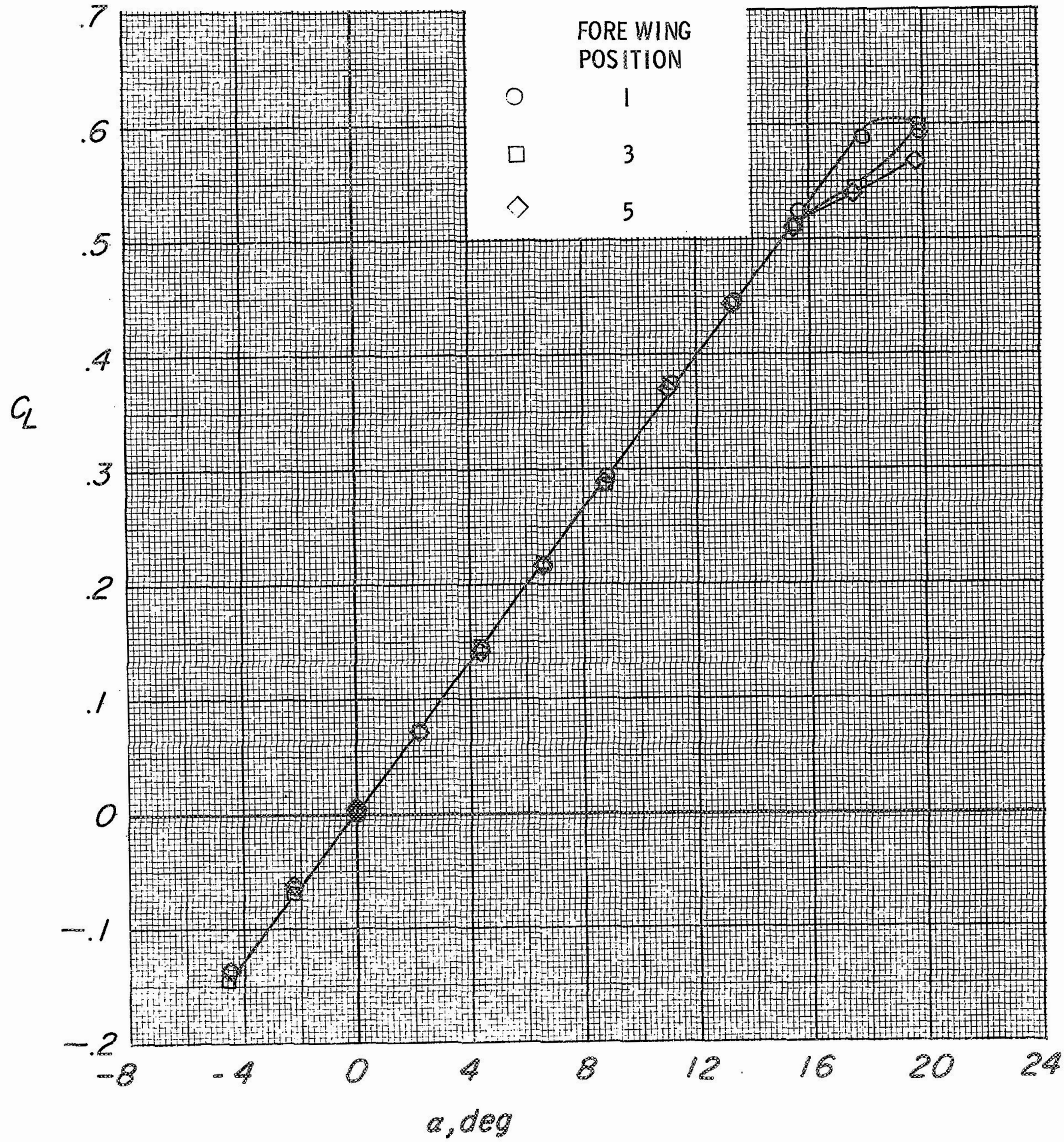

(b) Fore wing insert out.

Figure 8.- Continued.

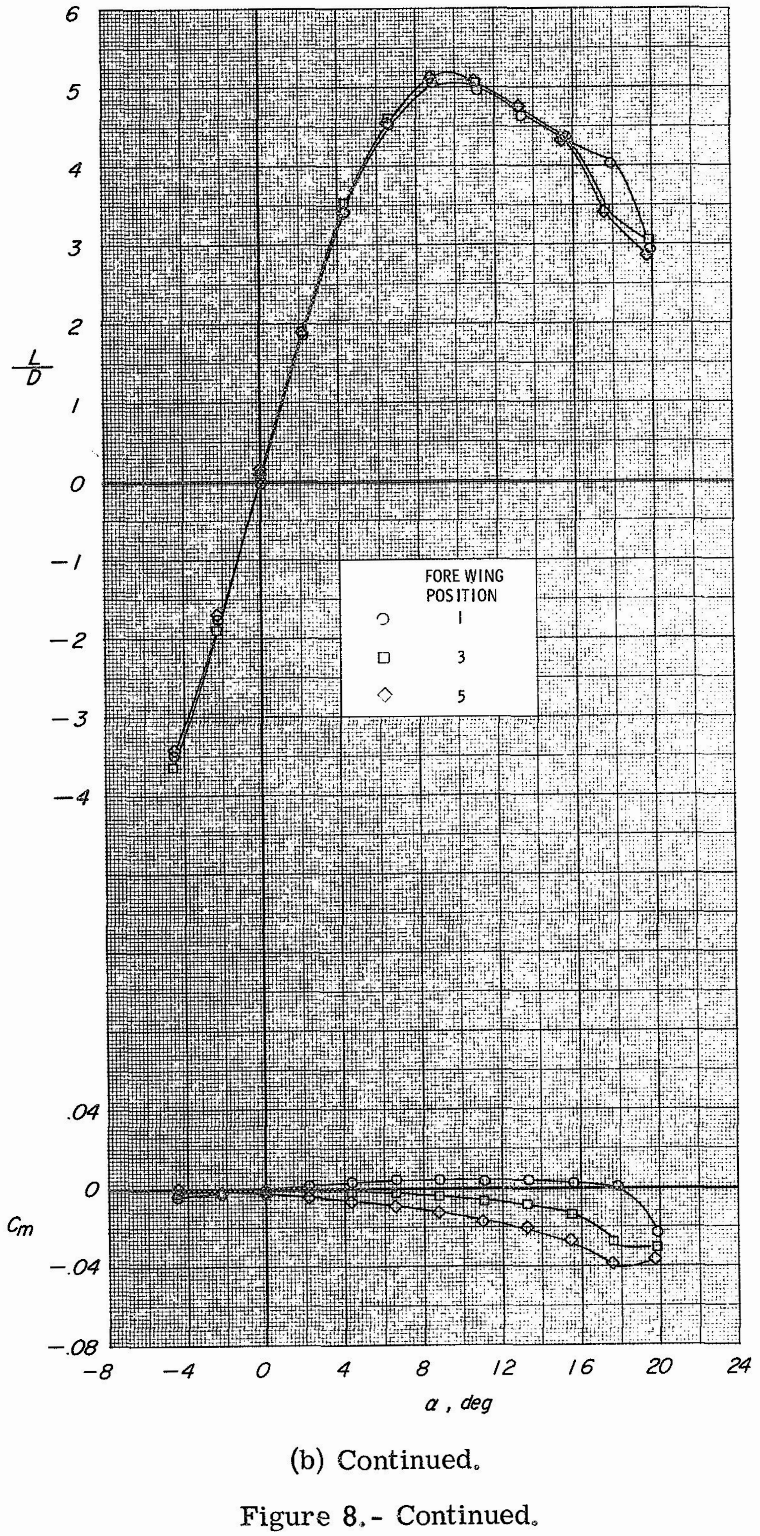

(b) Continued.

Figure 8.- Continued.

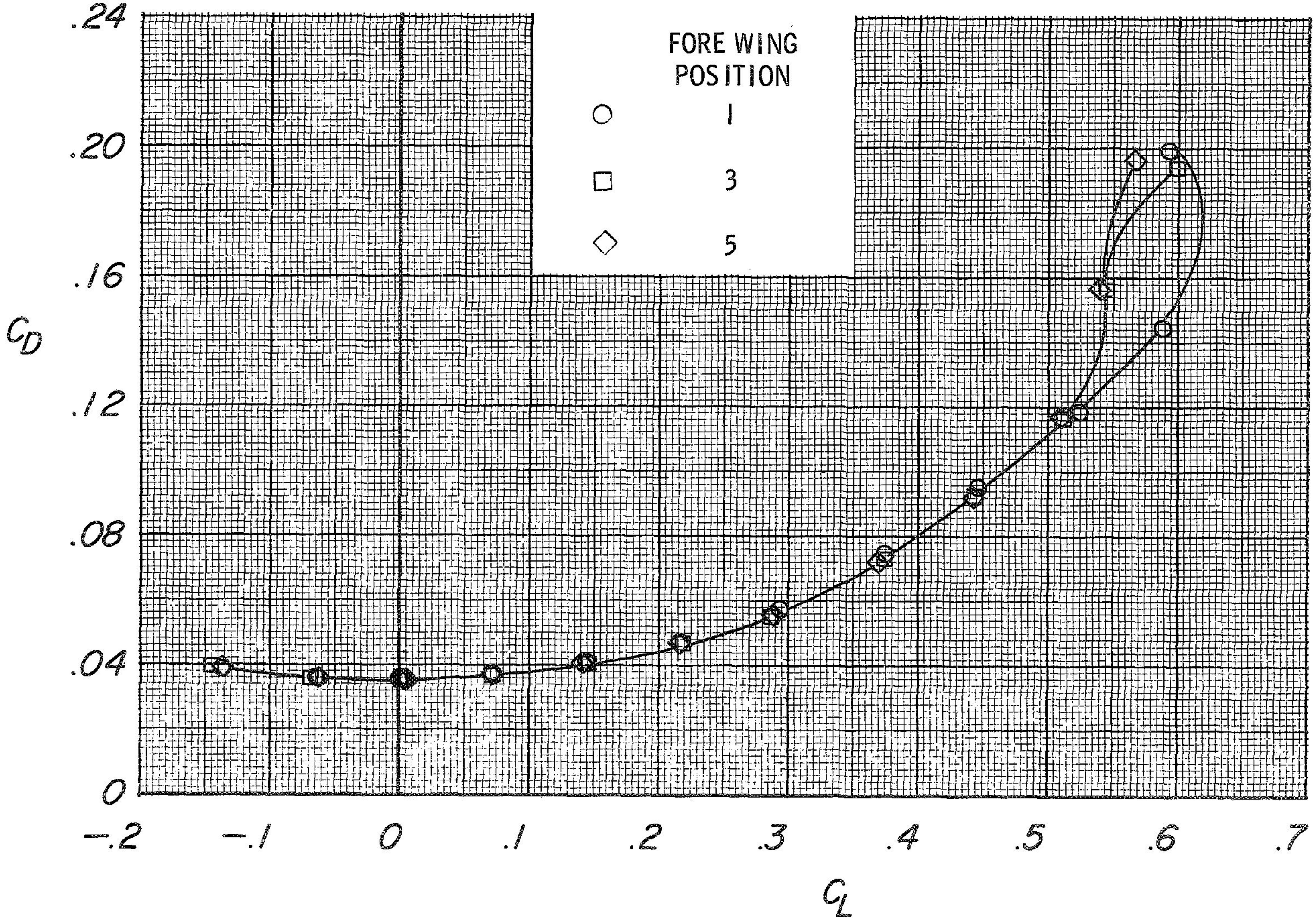

(b) Continued.

Figure 8.- Continued.

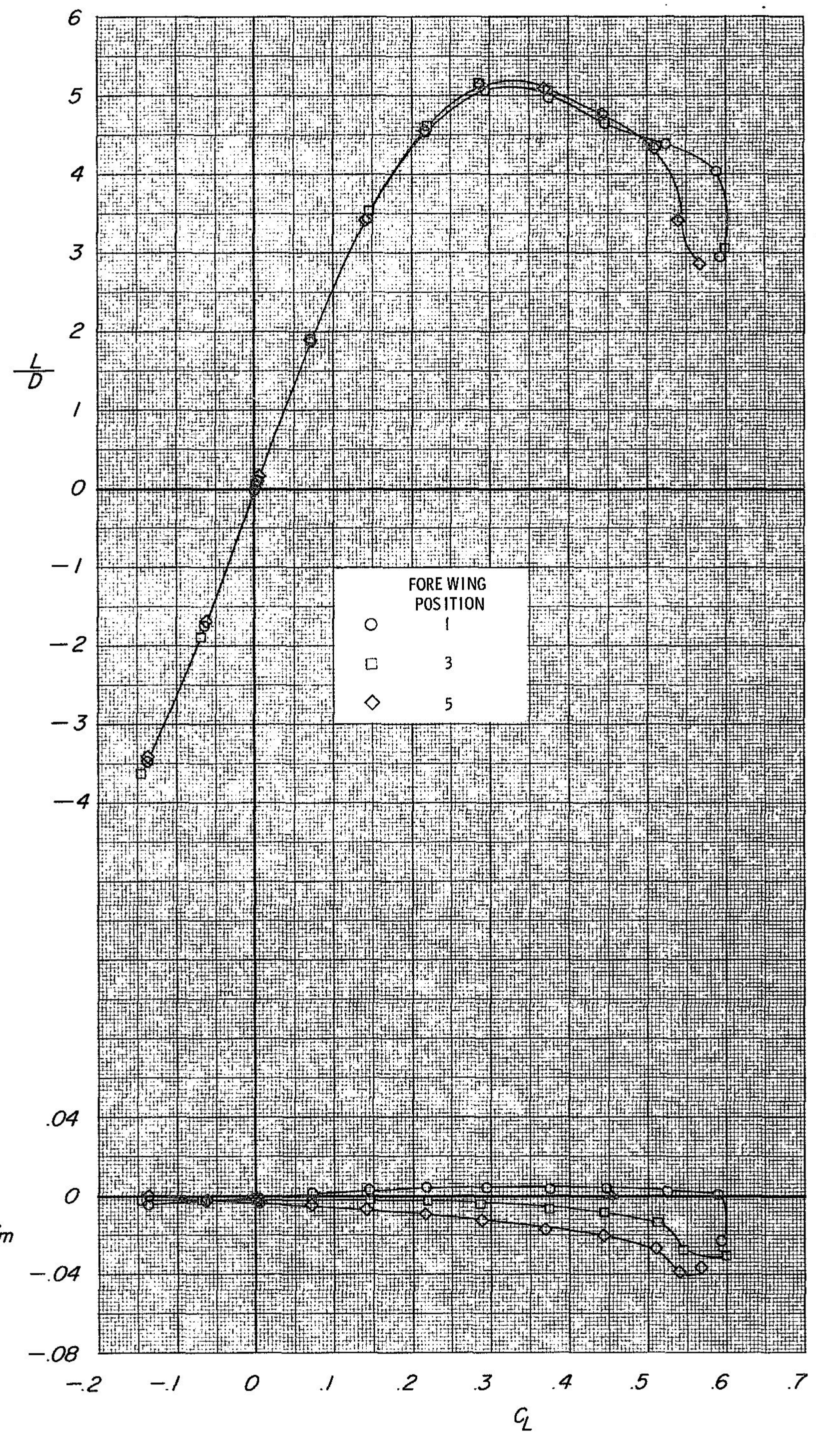

(b) Concluded.

Figure 8.- Concluded.

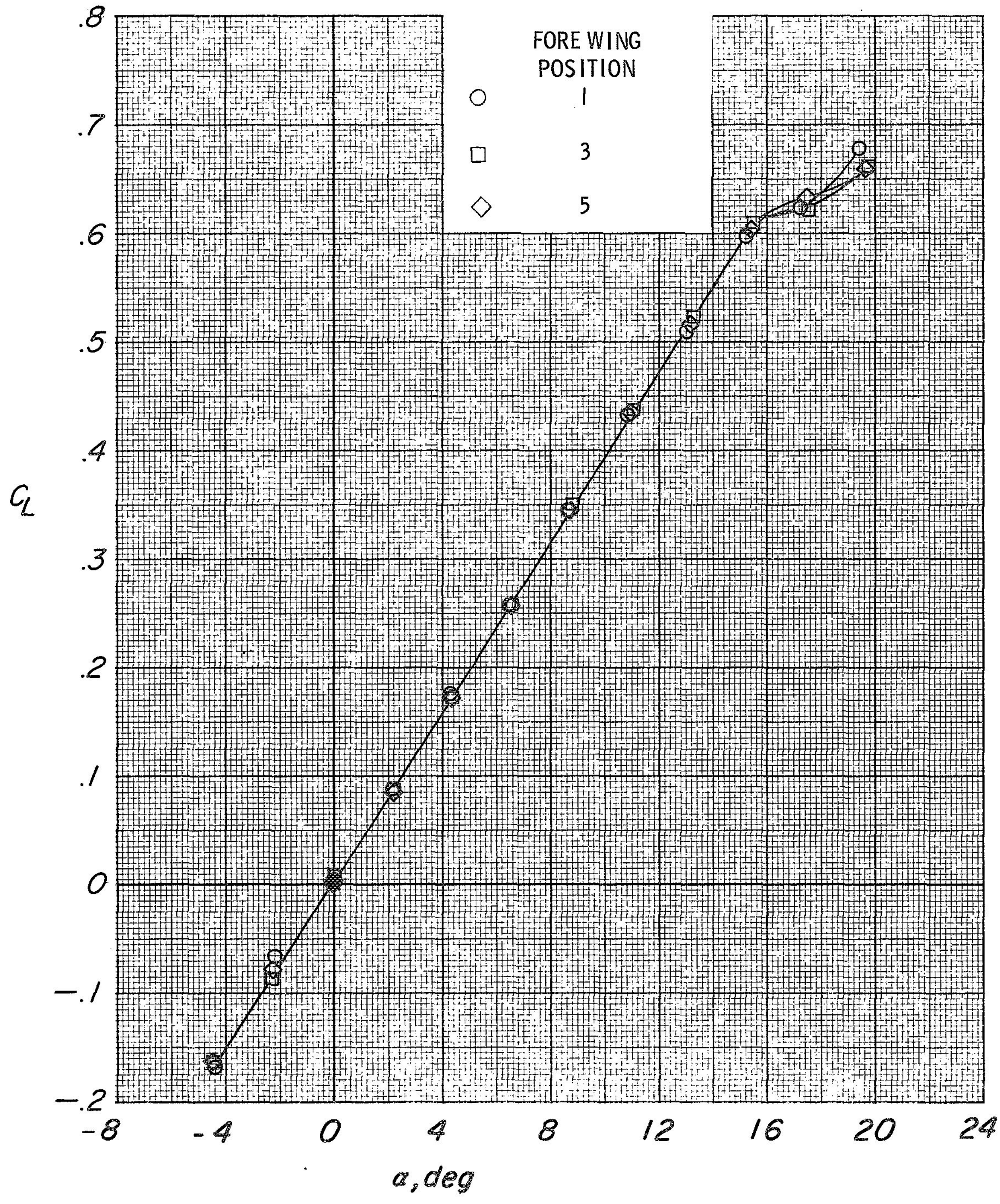

(a) Fore wing insert in.

Figure 9.- Effects of fore wing longitudinal position on longitudinal aerodynamic characteristics of model with intermediate-span wings (W_2) in high position. $R = 17.4 \times 10^6$; vertical tails on; $\Gamma_H = 0^o$.

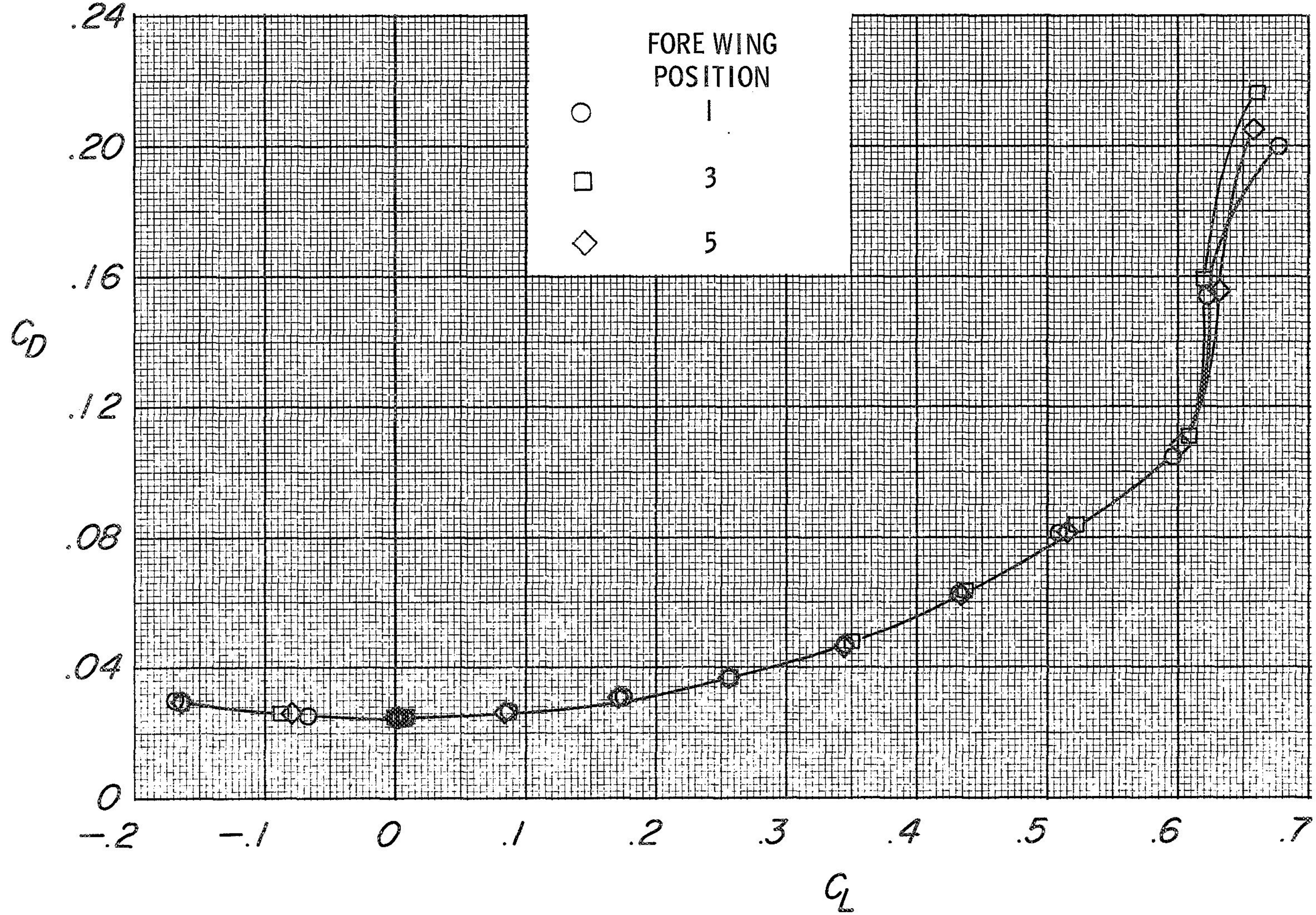

(a) Continued.

Figure 9.- Continued.

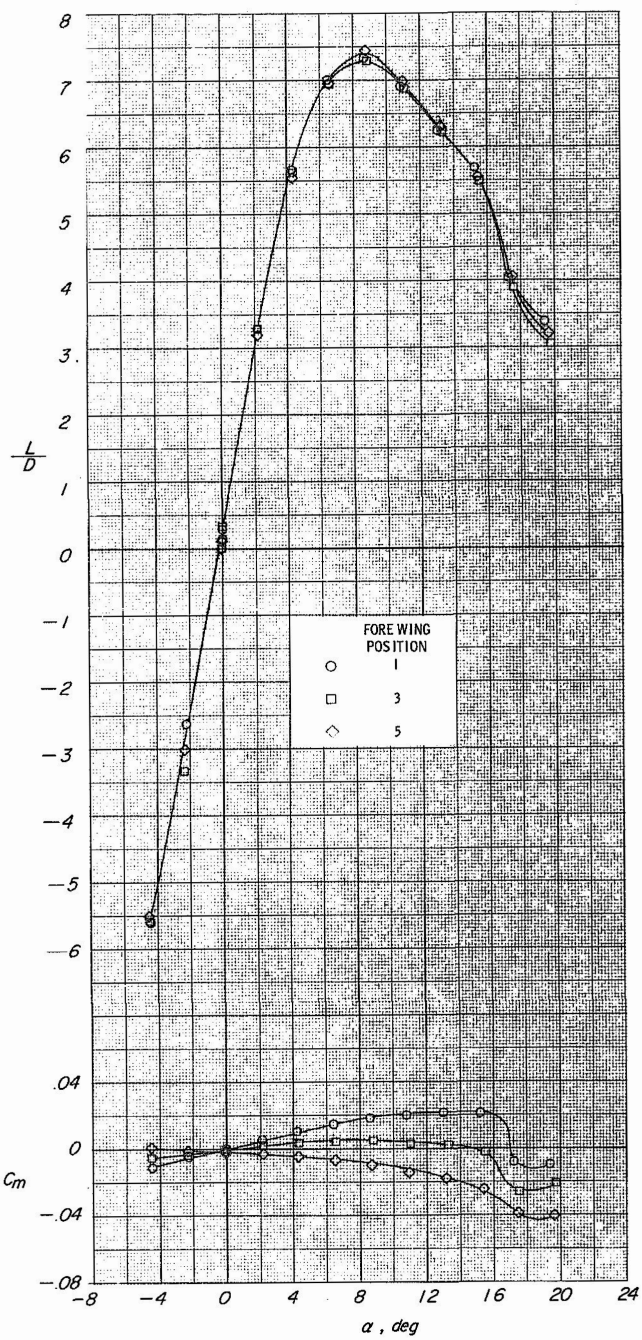

(a) Continued.

Figure 9.- Continued.

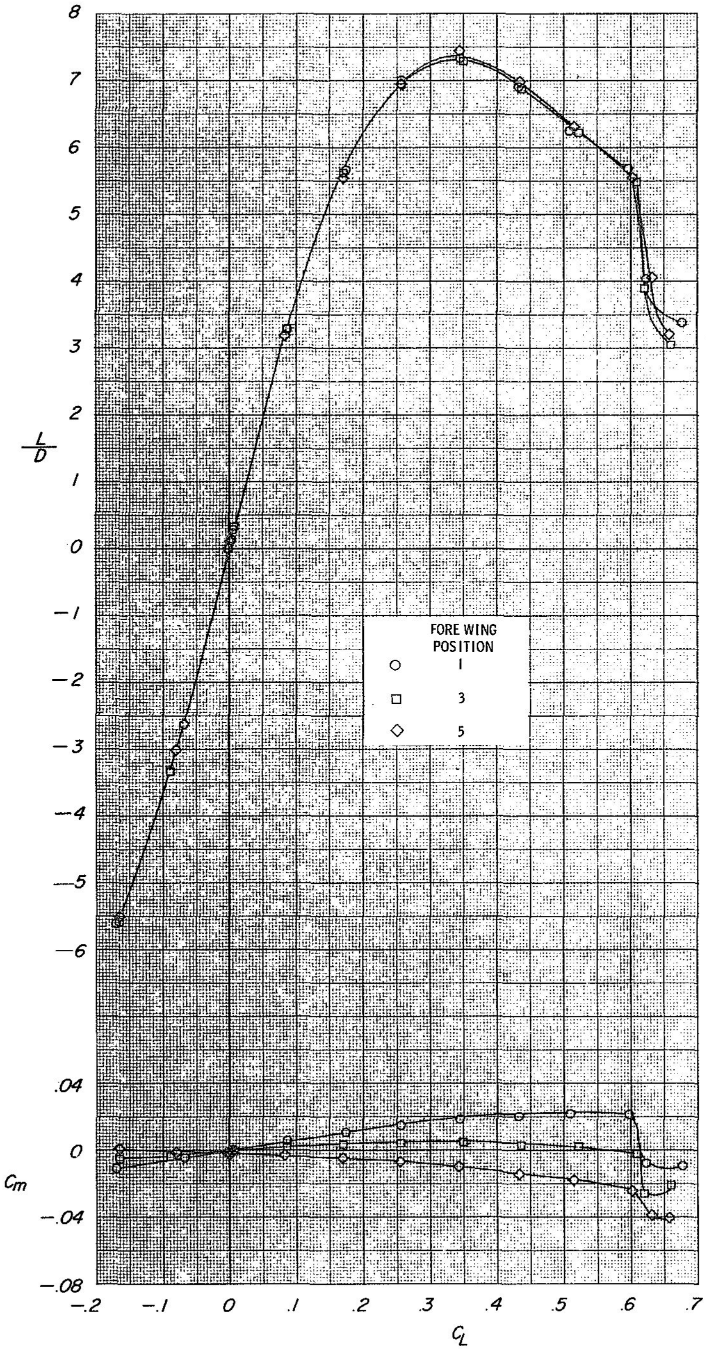

(a) Concluded.

Figure 9.- Continued.

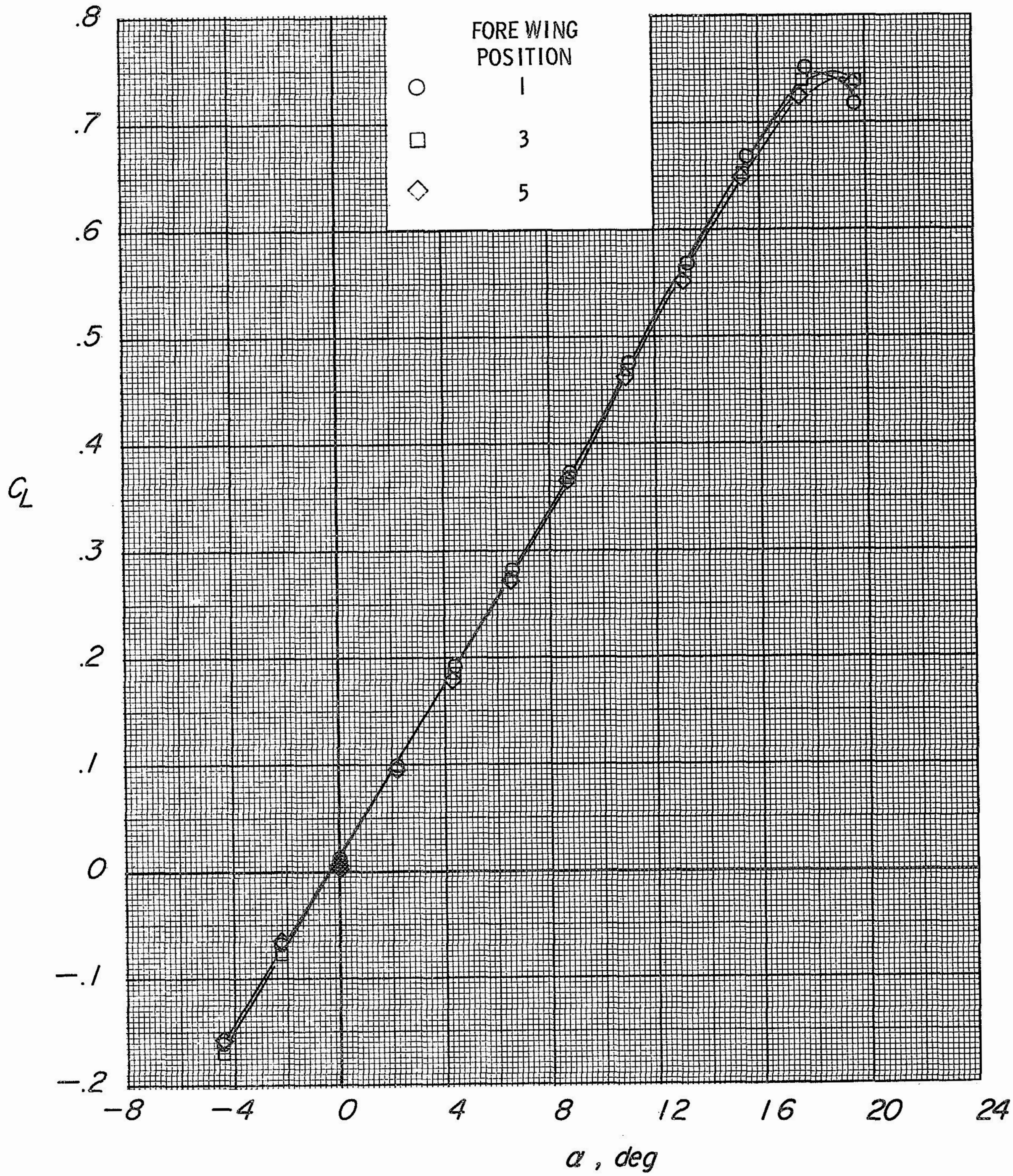

(b) Fore wing insert out.

Figure 9.- Continued.

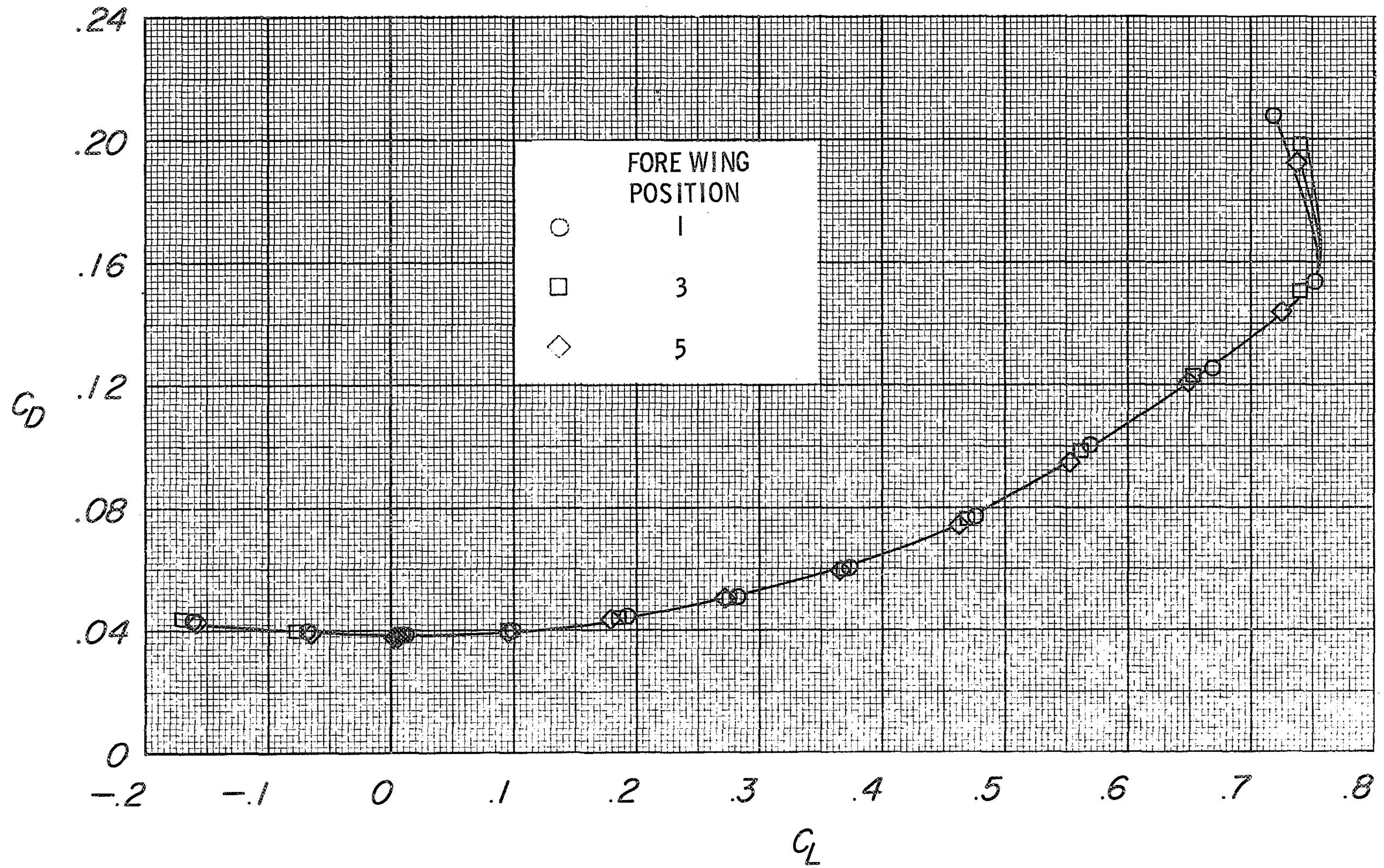

(b) Continued.

Figure 9.- Continued.

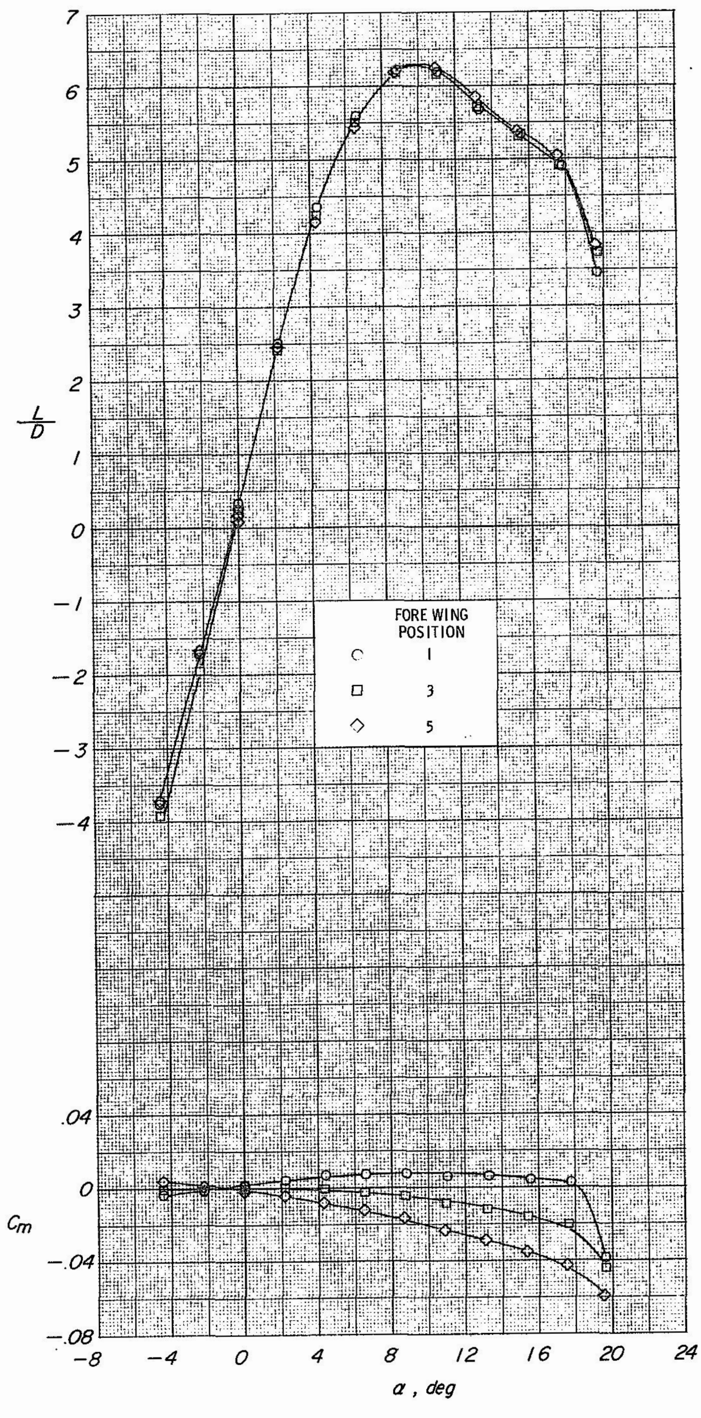

(b) Continued.

Figure 9.- Continued.

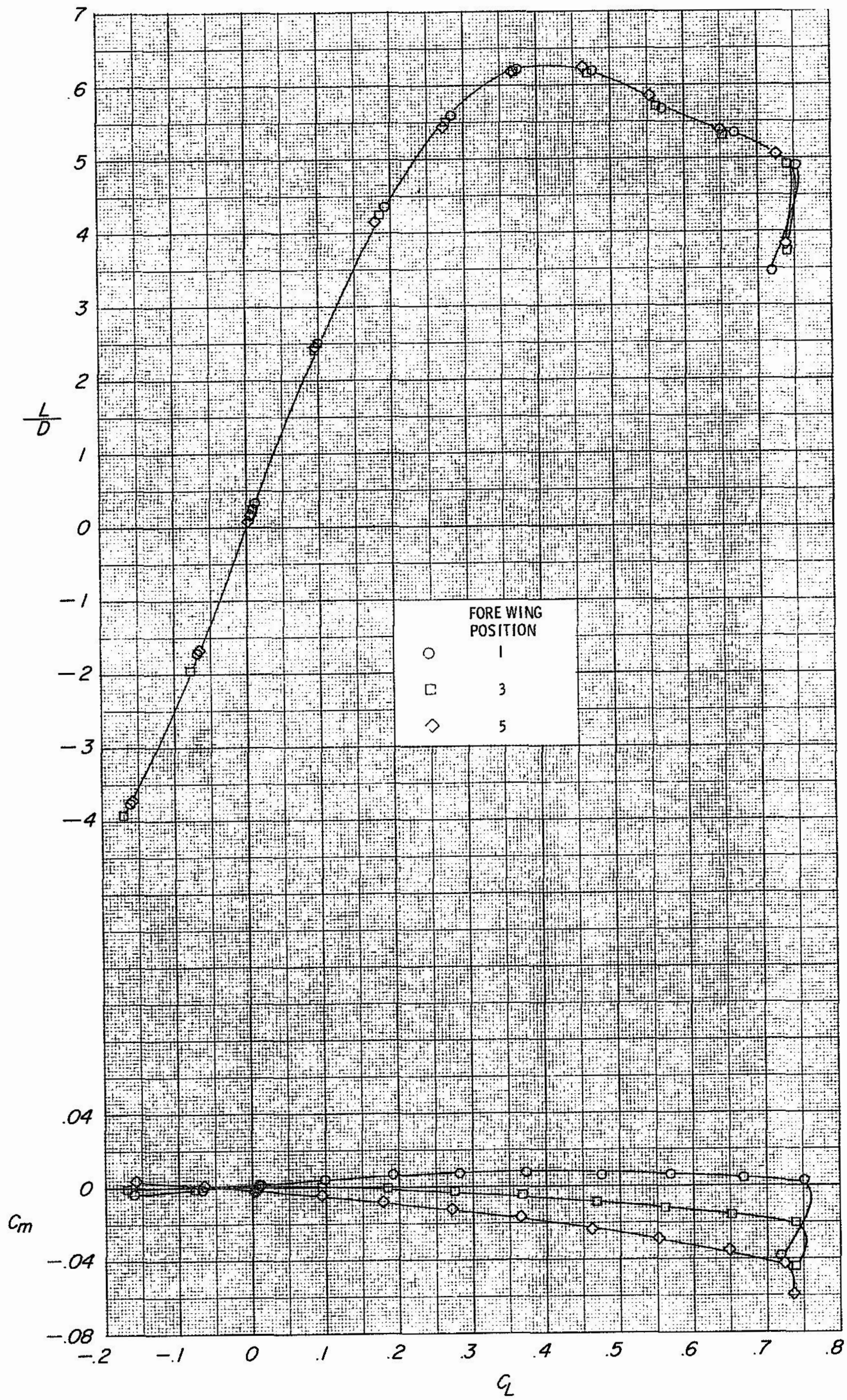

(b) Concluded.

Figure 9.- Concluded.

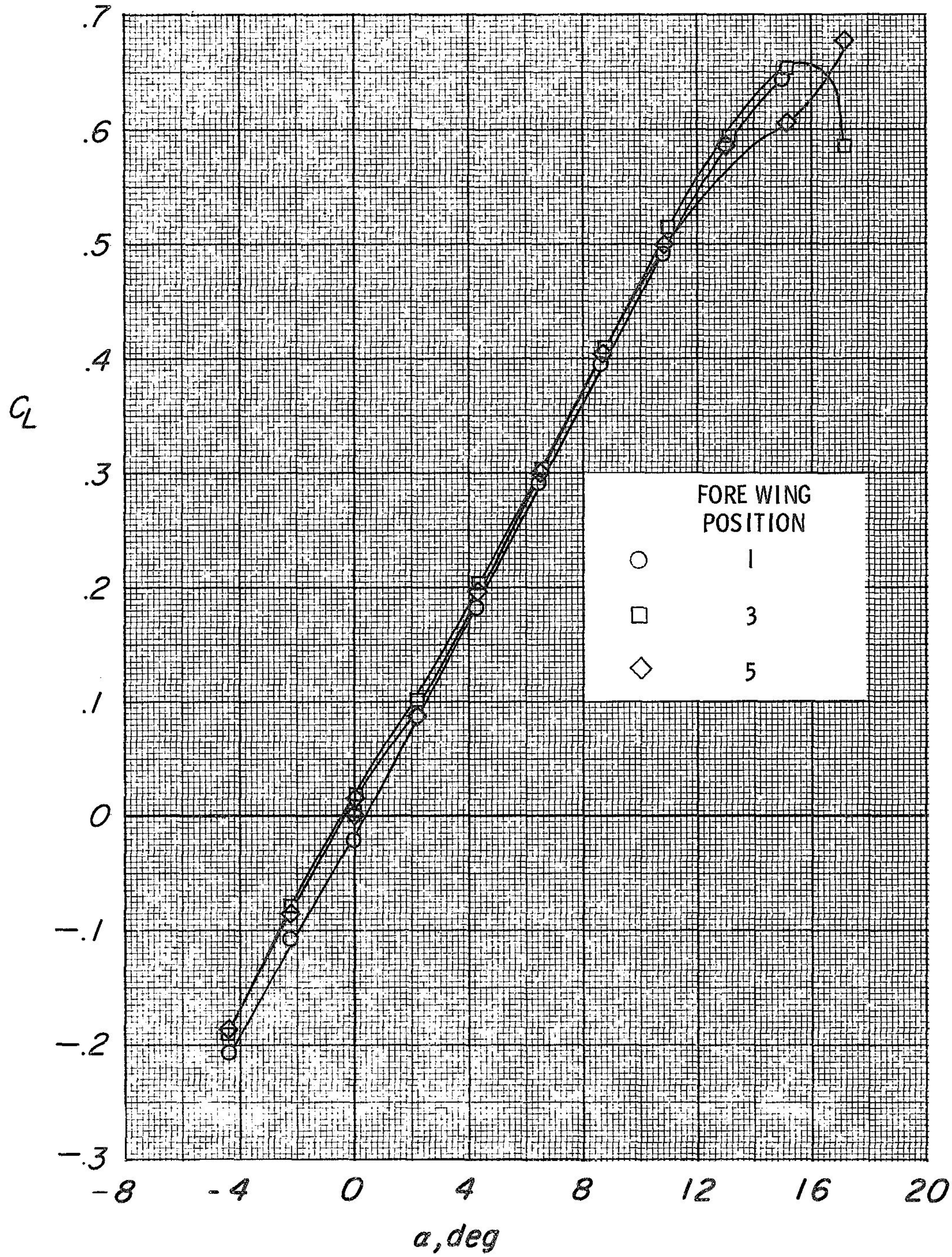

(a) Fore wing insert in.

Figure 10.- Effects of fore wing longitudinal position on longitudinal aerodynamic characteristics of model with maximum-span wings (W_3) in high position. $R = 10.4 \times 10^6$; vertical tails on; $\Gamma_H = 0^o$.

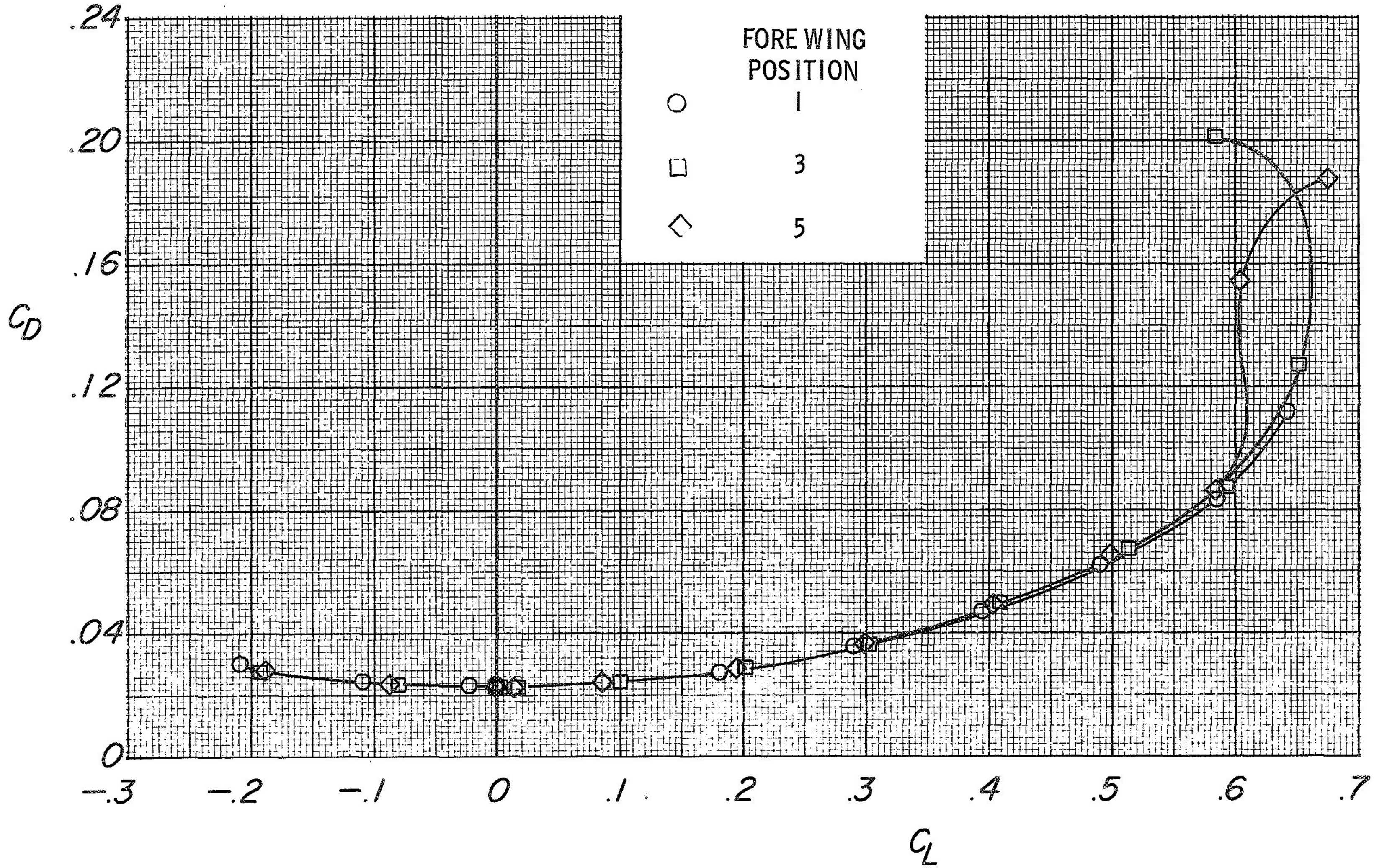

(a) Continued.

Figure 10.- Continued.

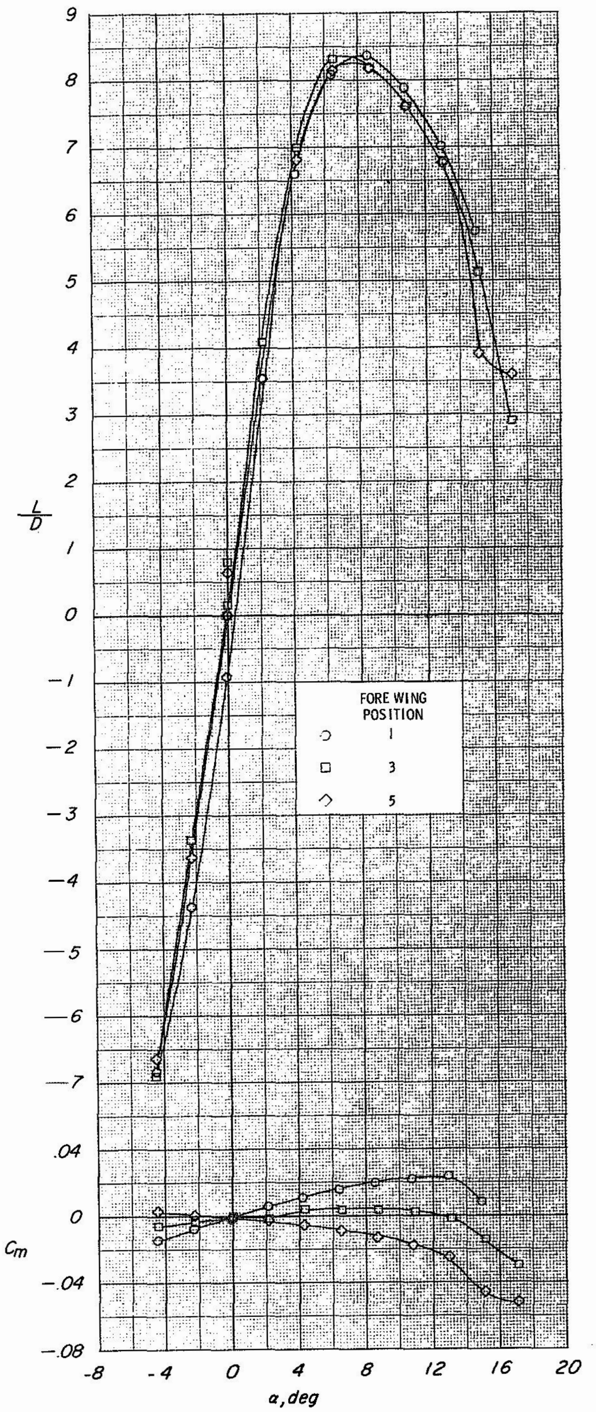

(a) Continued.

Figure 10.- Continued.

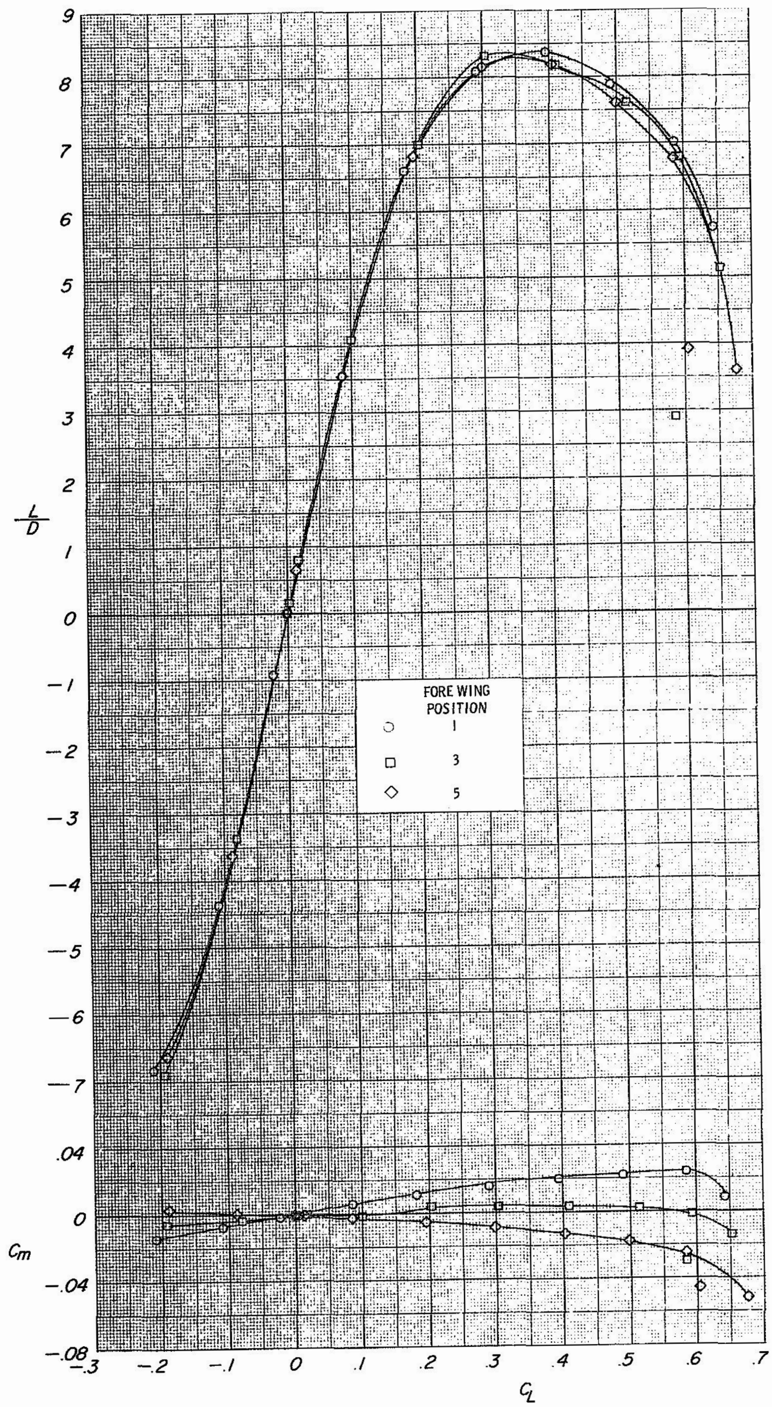

(a) Concluded.

Figure 10.- Continued.

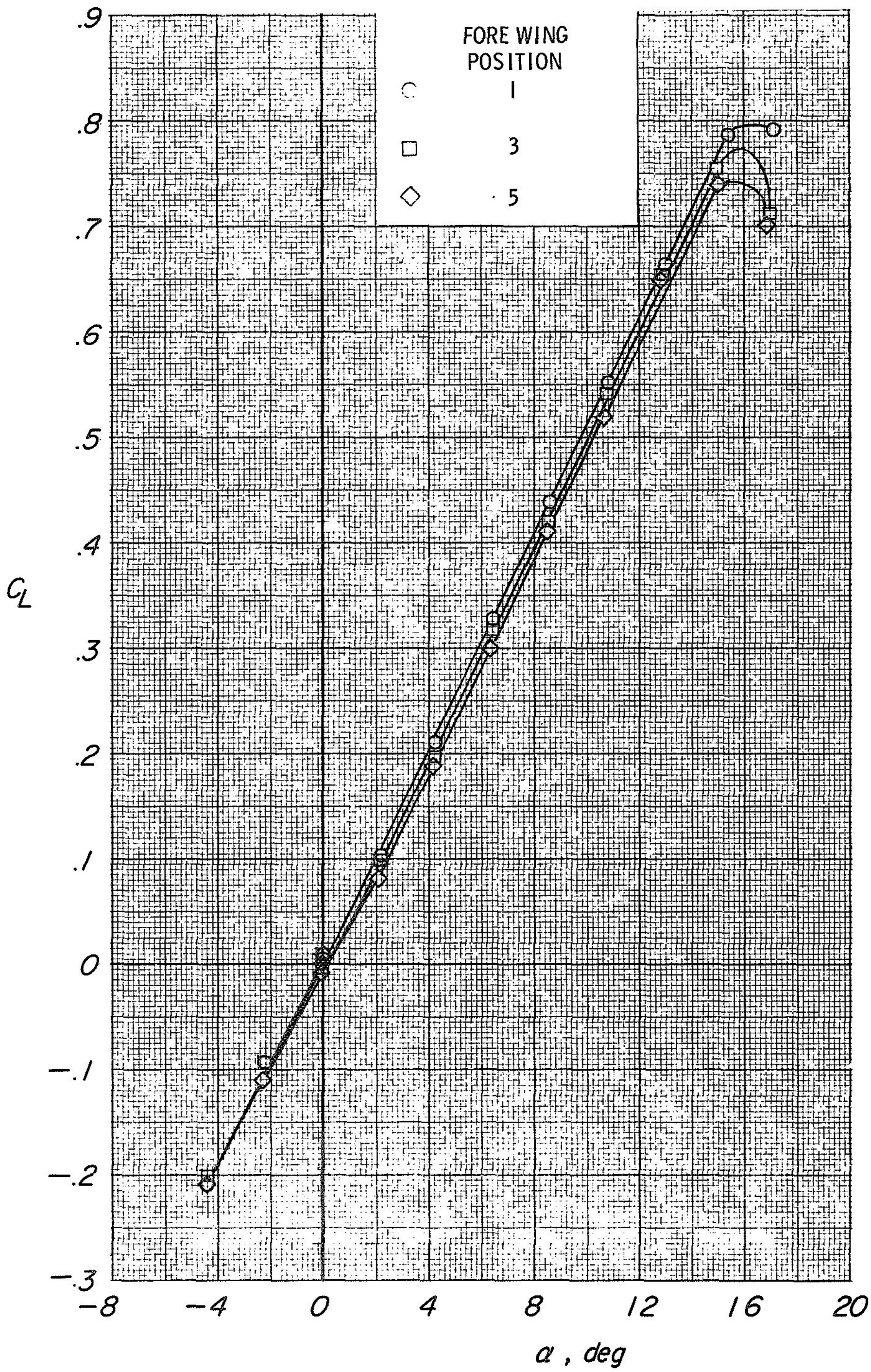

(b) Fore wing insert out.

Figure 10.- Continued.

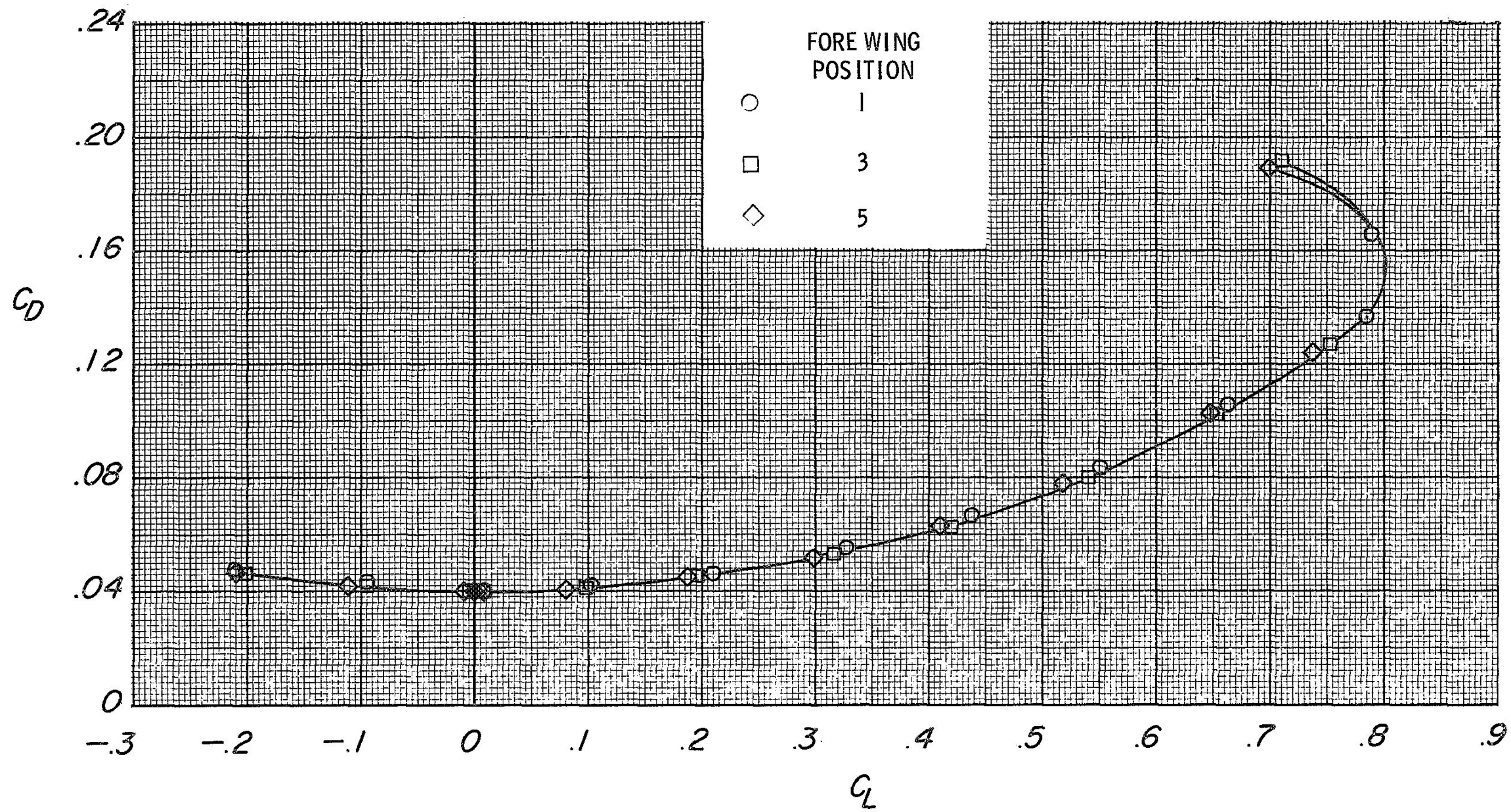

(b) Continued.

Figure 10.- Continued.

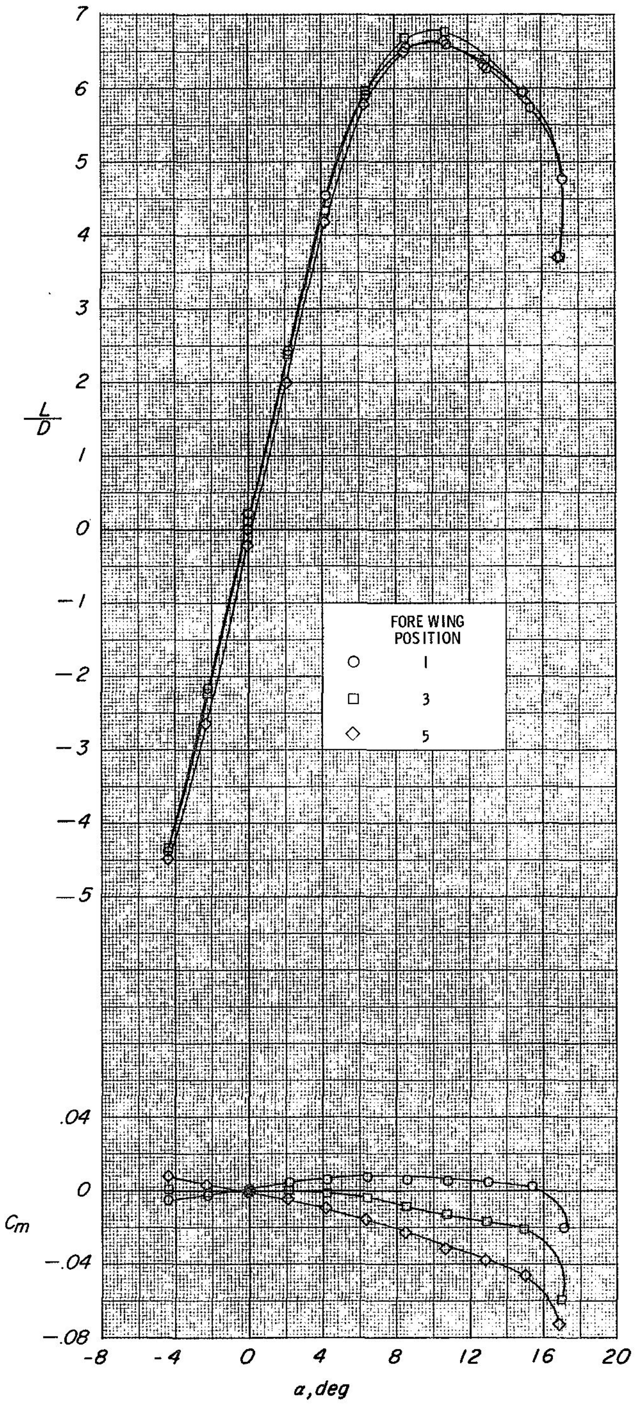

(b) Continued.

Figure 10.- Continued.

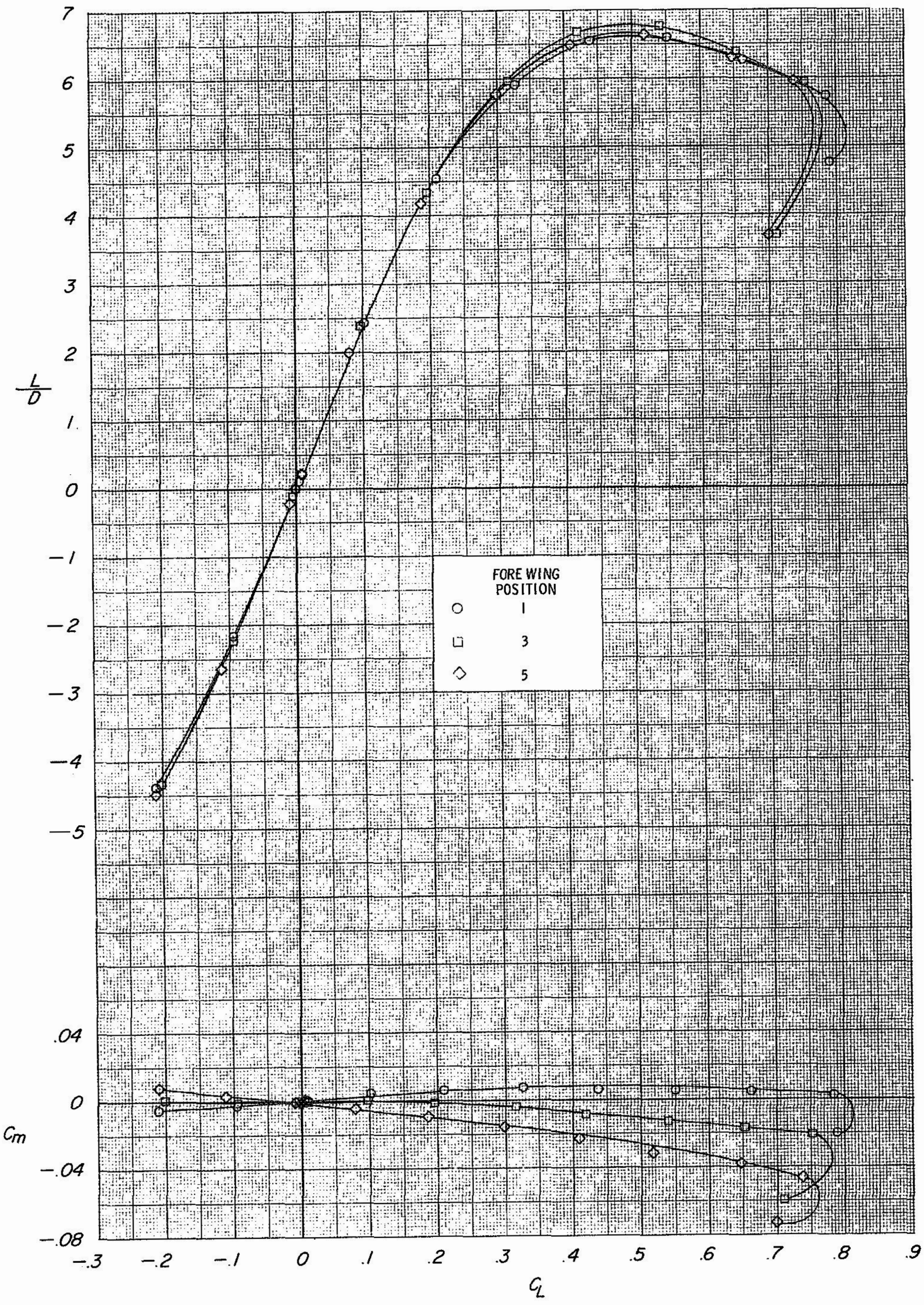

(b) Concluded.

Figure 10.- Concluded.

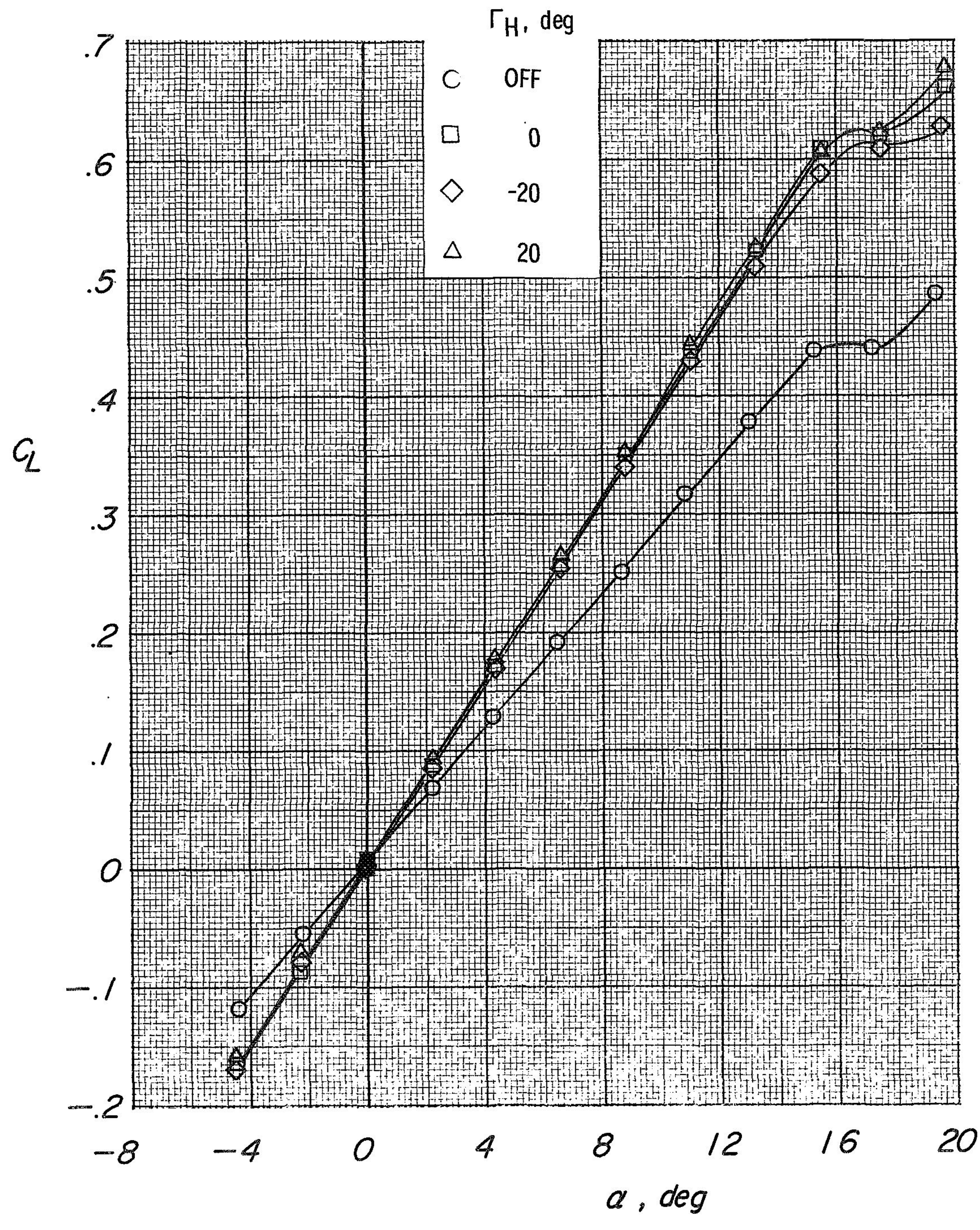

Figure 11.- Effects of horizontal stabilizers and stabilizer dihedral angle on longitudinal aerodynamic characteristics of model with intermediate-span wings (W_2) in high position. $R = 17.4 \times 10^6$; fore wing in longitudinal position 3; vertical tails on.

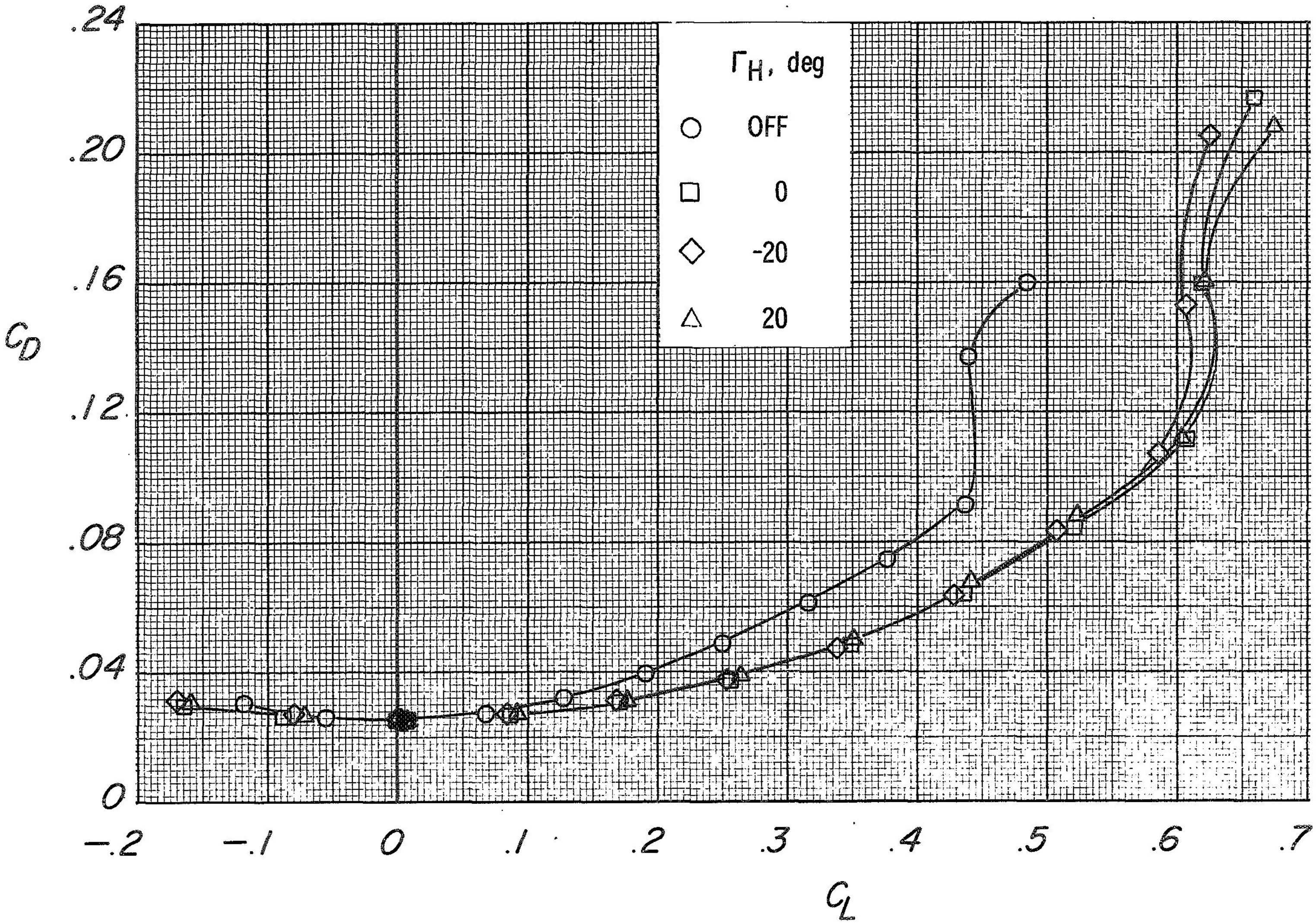

Figure 11.- Continued.

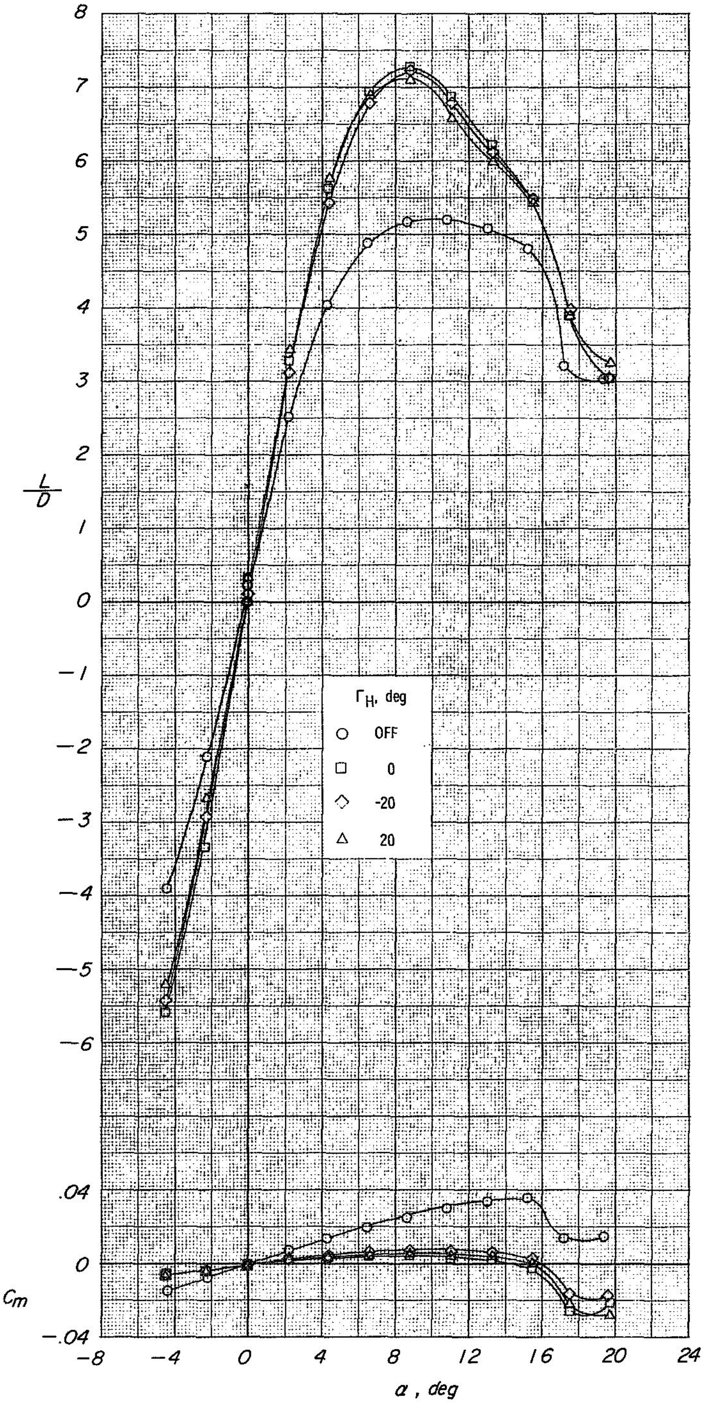

Figure 11.- Continued.

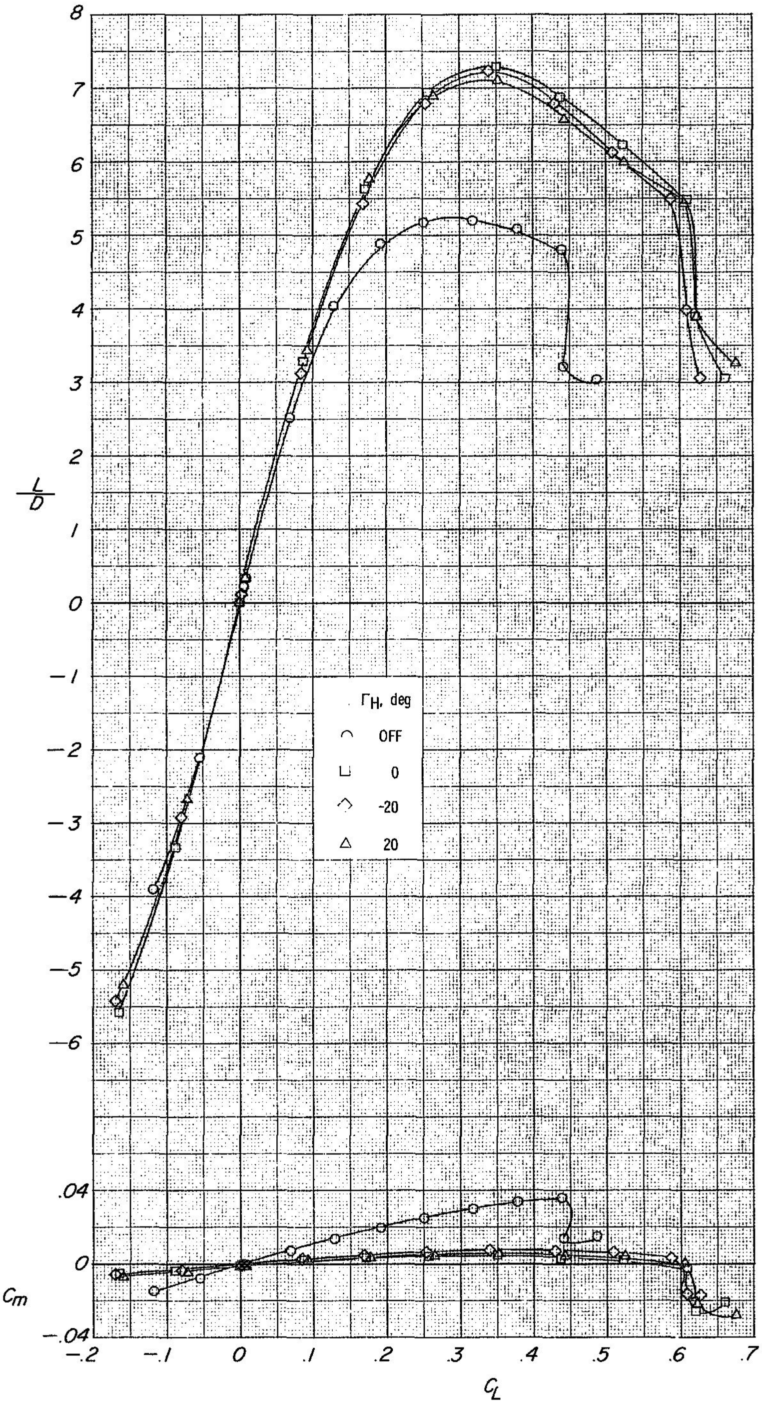

Figure 11.- Concluded.

NATIONAL AERONAUTICS AND SPACE ADMINISTRATION
WASHINGTON, D. C. 20546

OFFICIAL BUSINESS
PENALTY FOR PRIVATE USE $300

FIRST CLASS MAIL

POSTAGE AND FEES PAID
NATIONAL AERONAUTICS AN
SPACE ADMINISTRATION

POSTMASTER: If Undeliverable (Section 158
Postal Manual) Do Not Retur

"The aeronautical and space activities of the United States shall be conducted so as to contribute . . . to the expansion of human knowledge of phenomena in the atmosphere and space. The Administration shall provide for the widest practicable and appropriate dissemination of information concerning its activities and the results thereof."

—NATIONAL AERONAUTICS AND SPACE ACT OF 1958

NASA SCIENTIFIC AND TECHNICAL PUBLICATIONS

TECHNICAL REPORTS: Scientific and technical information considered important, complete, and a lasting contribution to existing knowledge.

TECHNICAL NOTES: Information less broad in scope but nevertheless of importance as a contribution to existing knowledge.

TECHNICAL MEMORANDUMS: Information receiving limited distribution because of preliminary data, security classification, or other reasons.

CONTRACTOR REPORTS: Scientific and technical information generated under a NASA contract or grant and considered an important contribution to existing knowledge.

TECHNICAL TRANSLATIONS: Information published in a foreign language considered to merit NASA distribution in English.

SPECIAL PUBLICATIONS: Information derived from or of value to NASA activities. Publications include conference proceedings, monographs, data compilations, handbooks, sourcebooks, and special bibliographies.

TECHNOLOGY UTILIZATION PUBLICATIONS: Information on technology used by NASA that may be of particular interest in commercial and other non-aerospace applications. Publications include Tech Briefs, Technology Utilization Reports and Technology Surveys.

Details on the availability of these publications may be obtained from:

SCIENTIFIC AND TECHNICAL INFORMATION OFFICE

NATIONAL AERONAUTICS AND SPACE ADMINISTRATION

Washington, D.C. 20546